August 27-28, 2024

Xinchang Zhang, Ph.D.

xinchang.zhang@inl.gov

Embedded Fiber Optic Sensors in Structural Materials for Sensing in Extreme Environments

Xinchang Zhang, Joshua Daw, Jorgen Rufner, Bibo Zhong, Austin Fleming, Zilong Hua

Idaho National Laboratory
Idaho Falls, ID, USA
xinchang.zhang@inl.gov

Idaho National Laboratory

Table of Contents

- 1. Background and Significance
- 2. Challenges with Current State-of-the-Art
- 3. Objectives
- 4. Research Methodology
  - 4.1. Fiber optic sensors embedding via EFAS
  - 4.2. Fiber integrity
  - 4.3. Fiber-matrix bonding
  - 4.4. Functionality of embedded fiber
  - 4.5. Mechanical properties
  - 4.6. Machinability
  - 4.7. Fiber properties after thermal cycling
- 5. Conclusions and Next Steps

1. Background and Significance

- Implementation of advanced sensors to provide online health monitoring capabilities is important to improve the performance of many advanced nuclear systems
- Fiber optic sensors are capable of multiplexed sensing of spatially distributed temperature and strain with high spatial resolution, and can offer stable measurement at extreme environments
- Embedding fiber optic sensors in metallic components has significant values in several industries

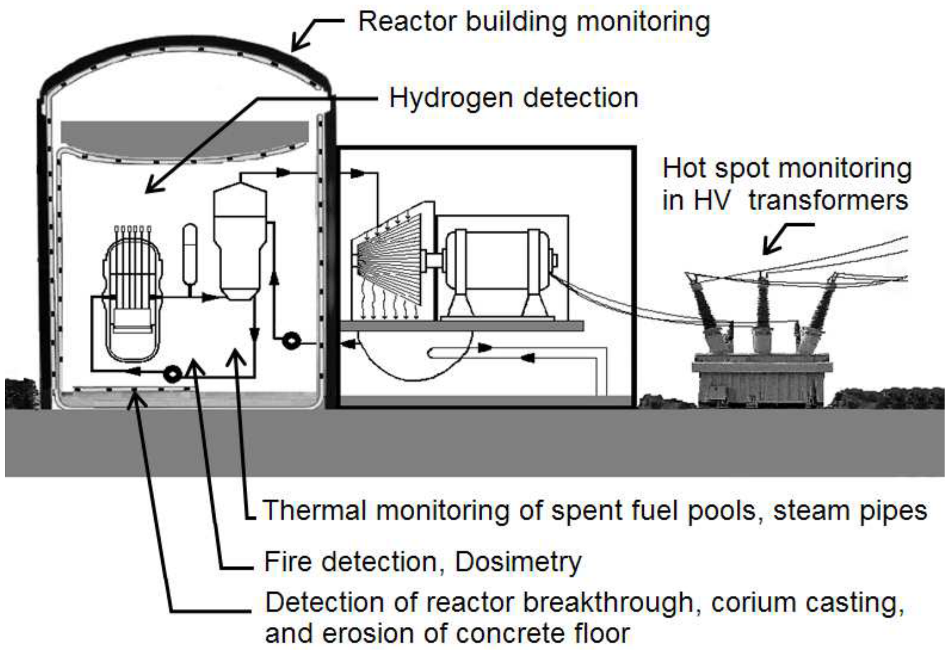

Application of fiber optic sensor in nuclear power plant [1]

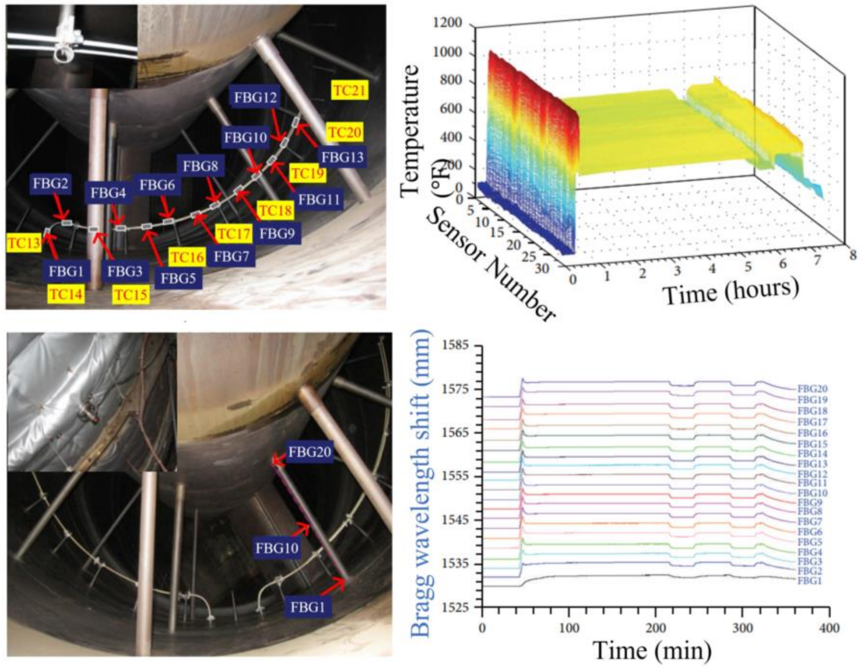

Optical fiber sensors installed in a gas turbine and test results [2]

[1] Ferdinand et al., Enhancing safety in nuclear power plant with optical fiber sensors, in Proc. Int. Conf. Fast Reactors Rel. Fuel Cycles, Safe Technol, vol. 46, no. 33, 2013.
[2] Xia et al., High-density fiber optical sensor and instrumentation for gas turbine operation condition monitoring, Journal of Sensors, vol. 2013, 2013.

2. Challenges with Current State-of-the Art

- Additive manufacturing (AM) has been recently explored to embed fiber optic sensors, including ultrasonic AM (UAM) and laser-based AM techniques
- For high-temperature materials, e.g., stainless steel and nickel-based alloys, a strong fiber/matrix bond is challenging due to an alloy's high strength and hardness
- Laser-based AM techniques have difficulties in embedding fibers due to the high temperature of the melt pool which damages the fiber, and therefore metal coatings on fiber are needed for protection. However, voids exist near the fiber due to inaccessibility of laser beam

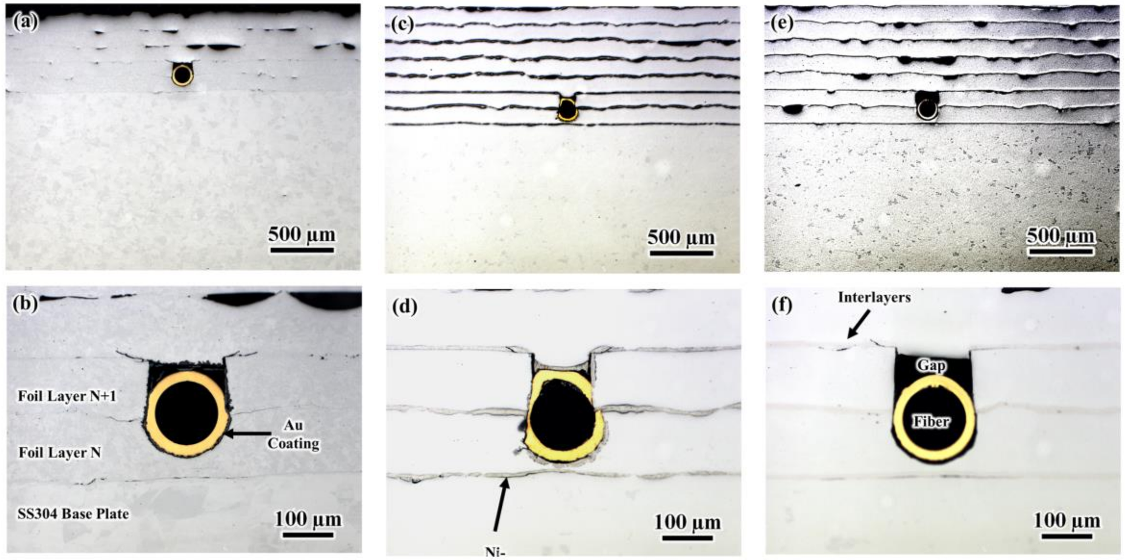

Optical microscopy images of embedded Au-coated fibers in (a, b) pure SS304 and in (c-f) Ni-plated SS304 with varied channel depths via UAM [3]

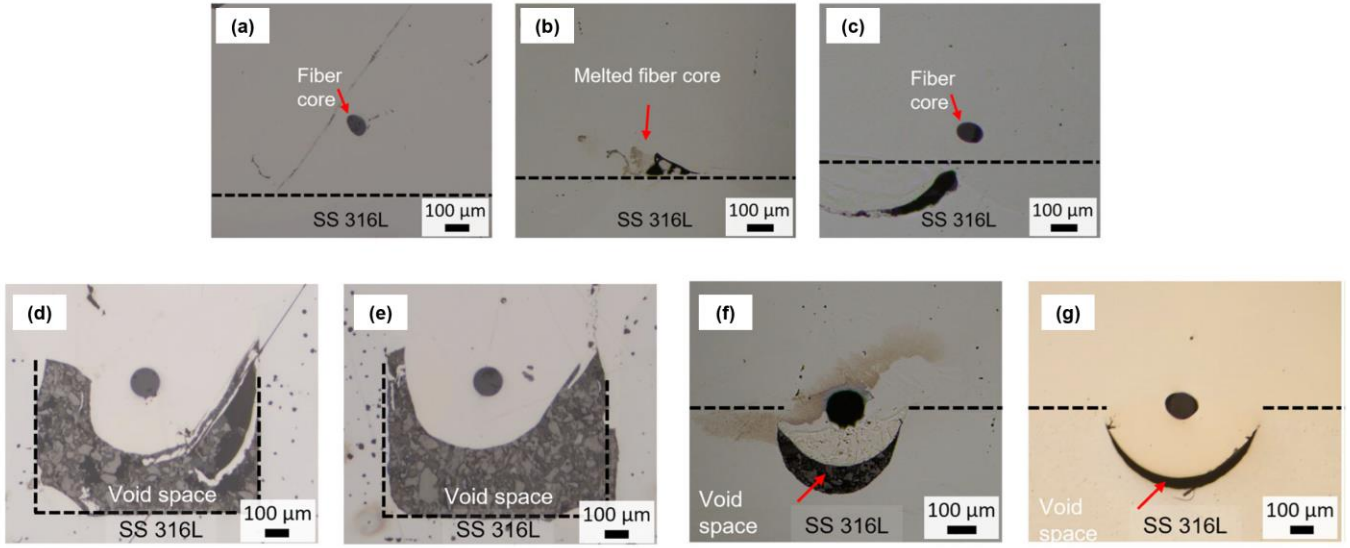

Optical microscopy images of embedded Ni-coated fibers in SS316L plates with (a-c) flat surface, (d, e) square groove, and (f, g) U groove using directed energy deposition [4]

[3] H.C. Hyer, D.C. Sweeney, C.M. Petrie, Functional fiber-optic sensors embedded in stainless steel components using ultrasonic additive manufacturing for distributed temperature and strain measurements, Additive Manufacturing 52 (2022) 102681
[4] S.I. Kim, H.Y. Jung, S. Yang, J. Yoon, H. Lee, W. Ryu, 3D Printing of a miniature turbine blade model with an embedded fibre Bragg grating sensor for high-temperature monitoring, Virtual and Physical Prototyping 17(2) (2022) 156-169.

3. Objectives

Objectives:

- Develop an SPS/EFAS-based advanced manufacturing technique to enable the integration of fiber optic sensors in high-temperature structural materials
- Achieve good bond between the embedded fiber and matrix
- Demonstrate the functionality of the embedded fiber optic sensors
- Obtain superior mechanical properties of the integrated materials
- Demonstrate machinability of the parts with embedded fibers

4. Research Methodology

1. Fabrication

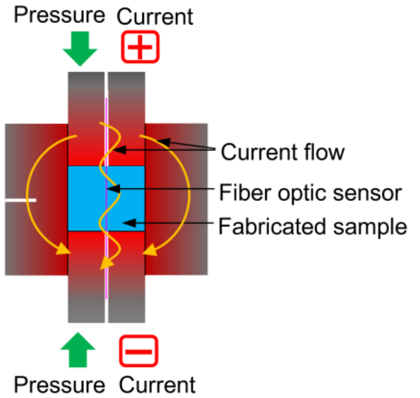

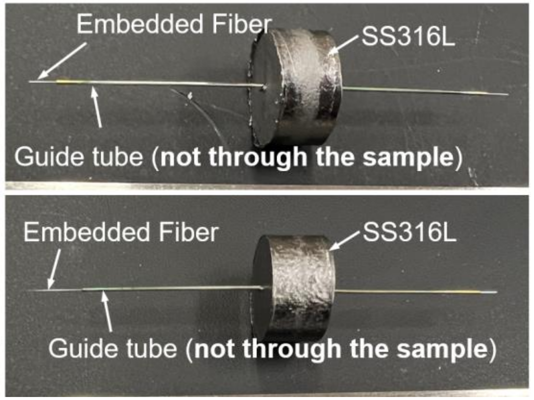

2. Process design and parameters

Technique: Development of EFAS process to embed fiber optic sensors

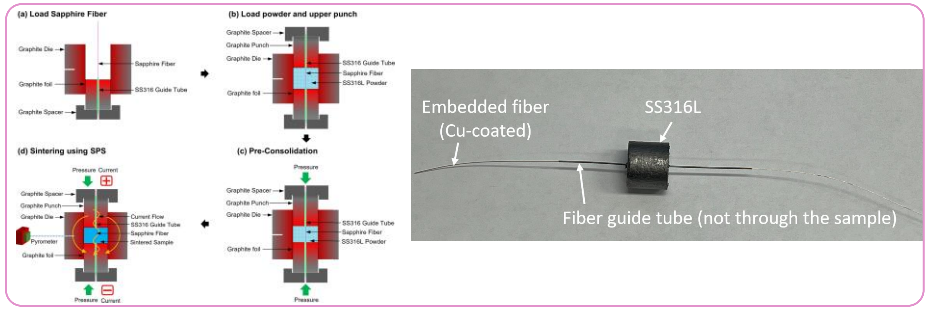

3. Fiber integrity and functionality

Measurement: Optical transmission test, OTDR test, XCT

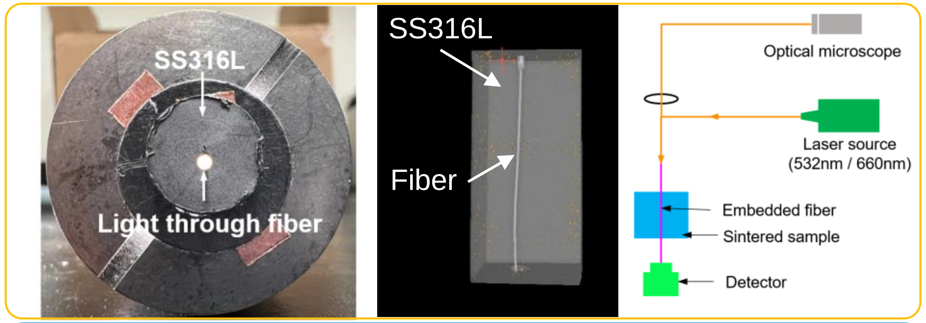

4. Fiber-matrix bonding quality

Characterization: Reveal the fiber-matrix bonding through X-CT, leak test, and advanced microscopy

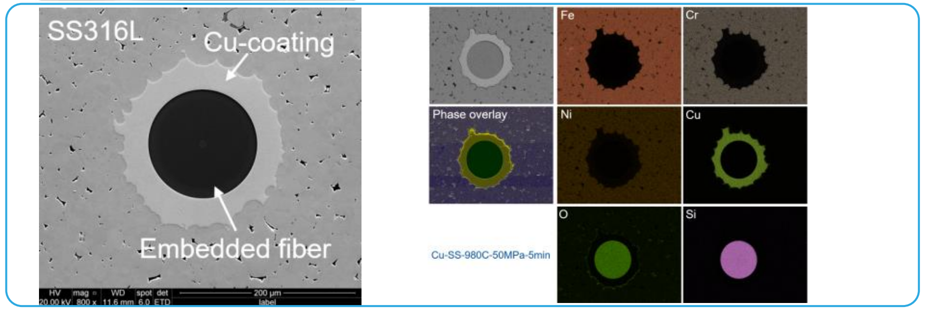

5. Properties after thermal cycling

Testing: Fiber functionality and fiber-matrix bonding after thermal cycling

6. Machinability

Machining: Demonstrate the machinability of the parts with embedded fibers

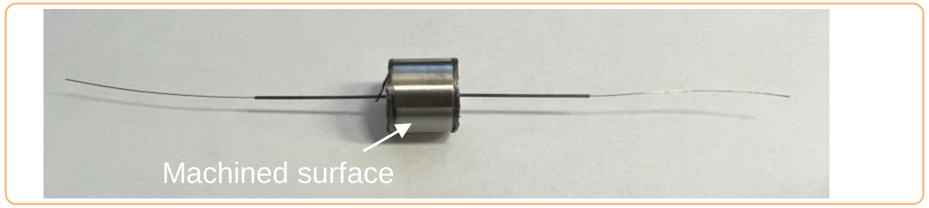

7. Mechanical properties

Testing: Understand the mechanical properties of the integrated materials with fiber optic sensors

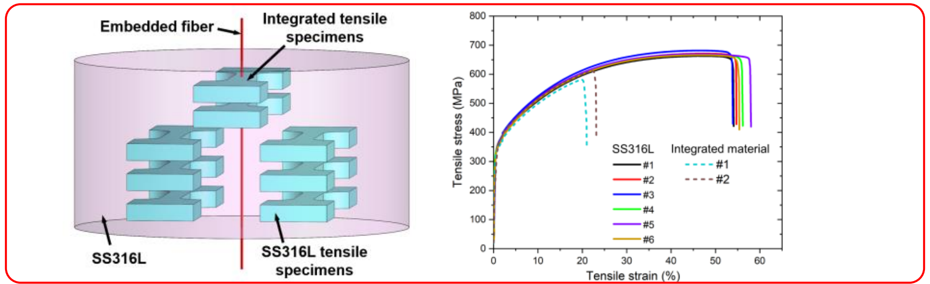

4.1. Fiber Optic Sensor Embedding via EFAS

- Sapphire fiber

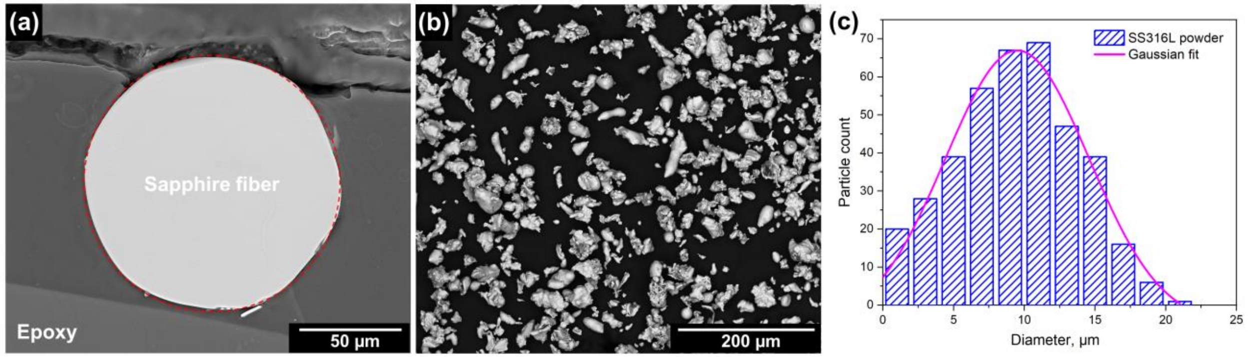

Specifications of SF125 sapphire optical fiber

Property	Value
Fiber diameter	125 µm
Fiber orientation	C-axis
Melting point	2072°C
Tensile strength	2200 MPa
Damage threshold	1.3 kJ/cm^2 @ 3µm
Numerical aperture	0.45
Attenuation	0.5 – 1.0 dB near-infrared (1m)
Bending loss	3% for 3 cm diameter loop

- SS316L powder

Chemical composition of SS316L

Element	Fe	Ni	Cr	Mo	Mn	Si	C	P	S
Wt. %	Bal.	12	17	2.5	2	0.75	0.03	0.045	0.03

- Fused silica fiber

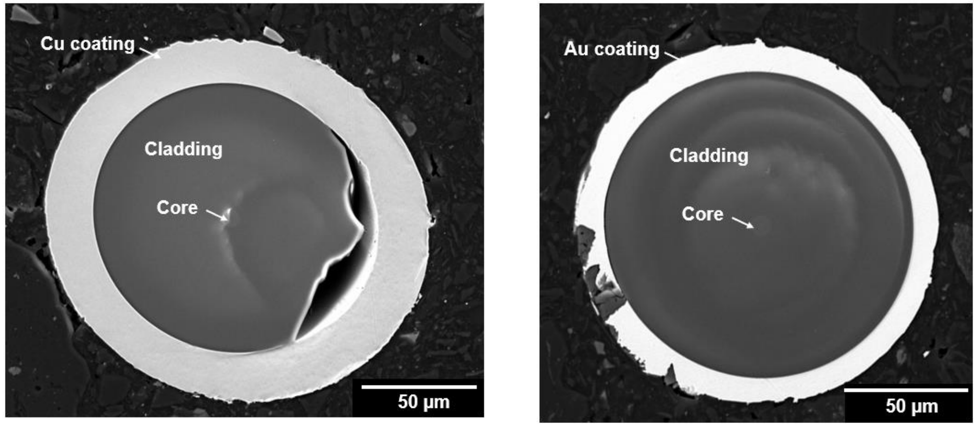

Specifications of Cu-coated and Au-coated fused silica fiber

Property	Fiber type	
	Cu-coated	Au-coated
Fiber diameter	165 µm (coating) 125 µm (cladding) 9 µm (core)	155 µm (coating) 125 µm (cladding) 9 µm (core)
Coating material	Copper alloy	Gold
Coating thickness	20~25 µm	10~15 µm
Wavelength	1300-1600 nm	1300-1600 nm
Melting point (coating)	~1085°C	~1064°C
Preform	Ge-doped core	Ge-doped core
Tensile strength	689.5 MPa	3.3 GPa
Numerical aperture	0.13	0.12
Attenuation	9.5 dB/km (800/1300 nm)	4 dB/Km (1310/1550nm)
Operating temperature	< 600°C	< 700°C

4.1. Fiber Optic Sensor Embedding via EFAS

- Fiber optic sensor embedding enabled by electric field assisted sintering (EFAS or SPS)

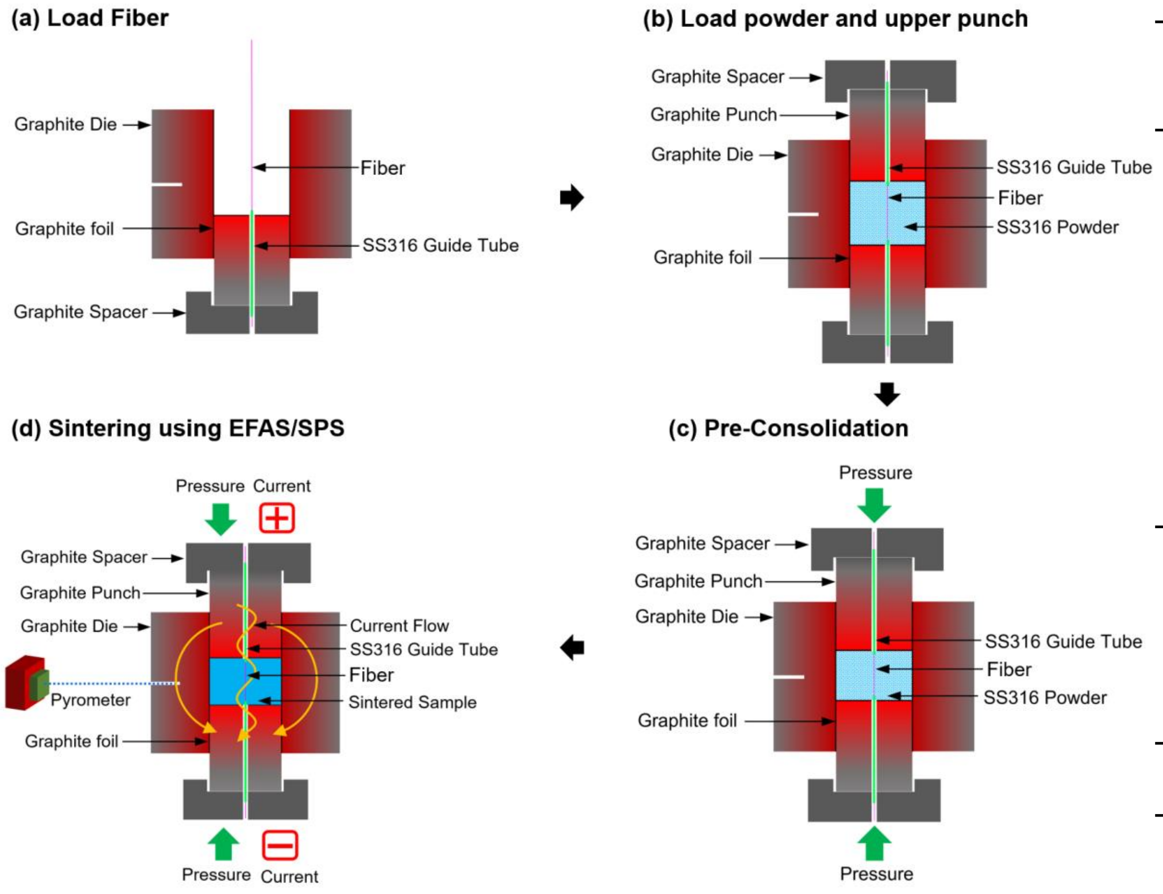

Schematics illustrating the proposed embedding process using EFAS

Parametric study in integrating fiber optic sensors in SS and nickel using EFAS

	Sample ID.	Temperature (°C)	Pressure (MPa)	Dwell time (min)
Sapphire fiber embedded in SS316L	SAF-SS-1000-10-5	1000	10	5
	SAF-SS-1000-20-5	1000	20	5
	SAF-SS-1000-50-5	1000	50	5
	SAF-SS-1000-50-10	1000	50	10
	SAF-SS-1050-50-5	1050	50	5
	SAF-SS-1050-50-10	1050	50	10
	SAF-SS-1100-10-5	1100	10	5
	SAF-SS-1100-20-5	1100	20	5
	SAF-SS-1100-50-5	1100	50	5
	SAF-SS-1150-20-5	1150	20	5
	SAF-SS-1150-50-5	1150	50	5
Cu-coated fiber embedded in SS316L	CuF-SS-800-40-5	800	40	5
	CuF-SS-900-40-5	900	40	5
	CuF-SS-980-40-5	980	40	5
	CuF-SS-980-50-5	980	50	5
	CuF-SS-980-50-10	980	50	10
	CuF-SS-980-60-10	980	60	10
Cu-coated fiber embedded in Ni	CuF-Ni-900-50-5	900	50	5
	CuF-Ni-980-50-5	980	50	5
Au-coated fiber embedded in SS316L	AuF-SS-800-40-5	800	40	5
	AuF-SS-900-40-5	900	40	5
	AuF-SS-980-40-5	980	40	5
	AuF-SS-980-40-5	980	40	5

X. Zhang et al. "Integrating fiber optic sensors into metallic components for sensing in harsh environments", Optics & Laser Technology, 170, 110118, 2024.

4.2. Fiber Integrity

- Embedded sapphire fiber
- Fiber integrity: successful transmission of light through the embedded sapphire fibers integrated into SS316L fabricated at all the conditions
- X-CT reveals good fiber integrity

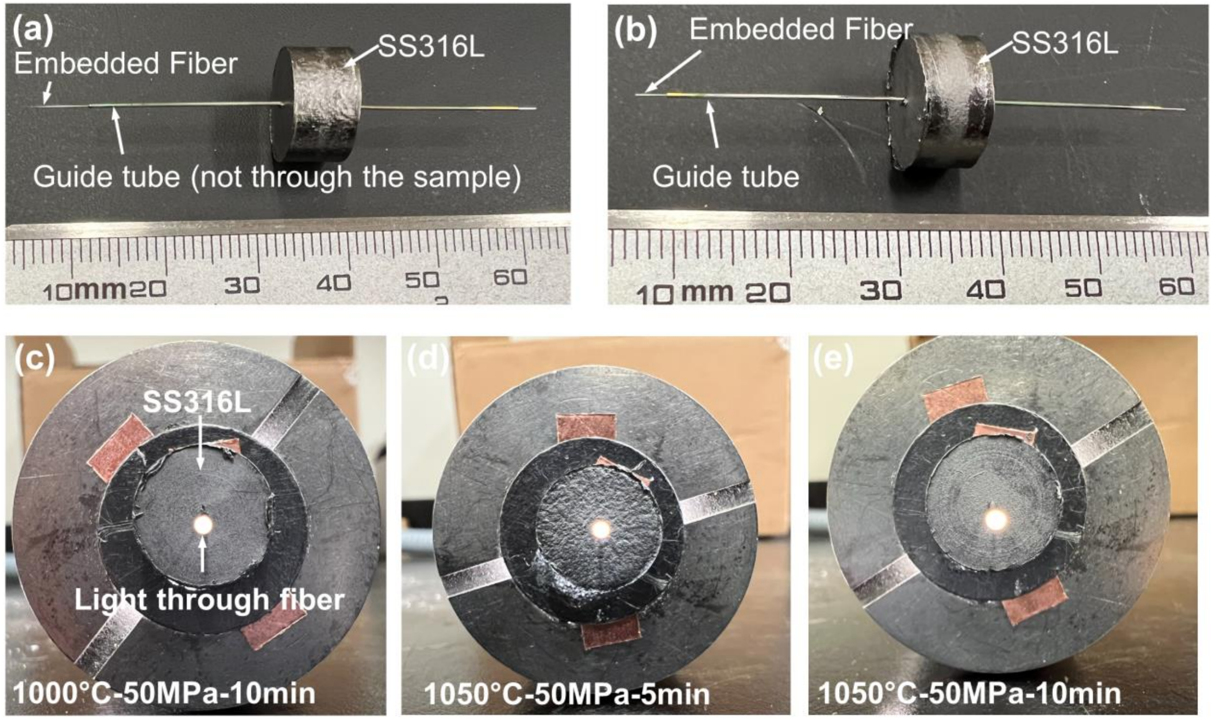

Images of SS316L with integrated fiber made at (a) 1000°C-20MPa-5min and (b) 1050°C-50MPa-5min. (c-d) Inspection of light through the fiber in samples made at varied conditions

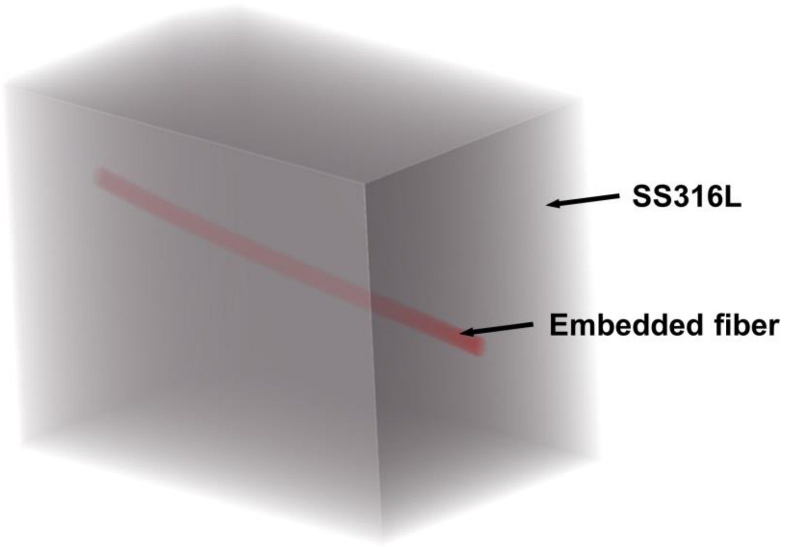

An XCT rendered image of a sub volume of the sample with embedded sapphire optical fiber (SAF-SS-1100-50-5).

4.2. Fiber Integrity

- Embedded fused silica fiber
- Fiber integrity: successful transmission of light through the embedded silica fibers integrated into SS316L fabricated at all the conditions
- X-CT reveals good fiber integrity

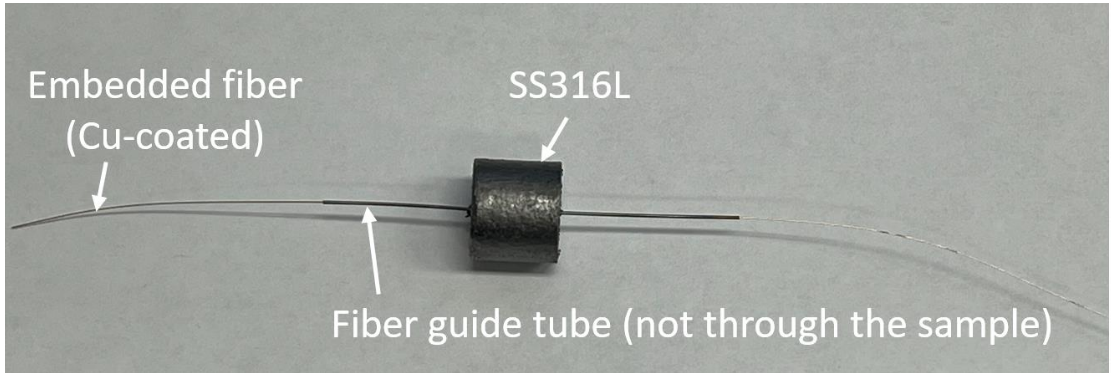

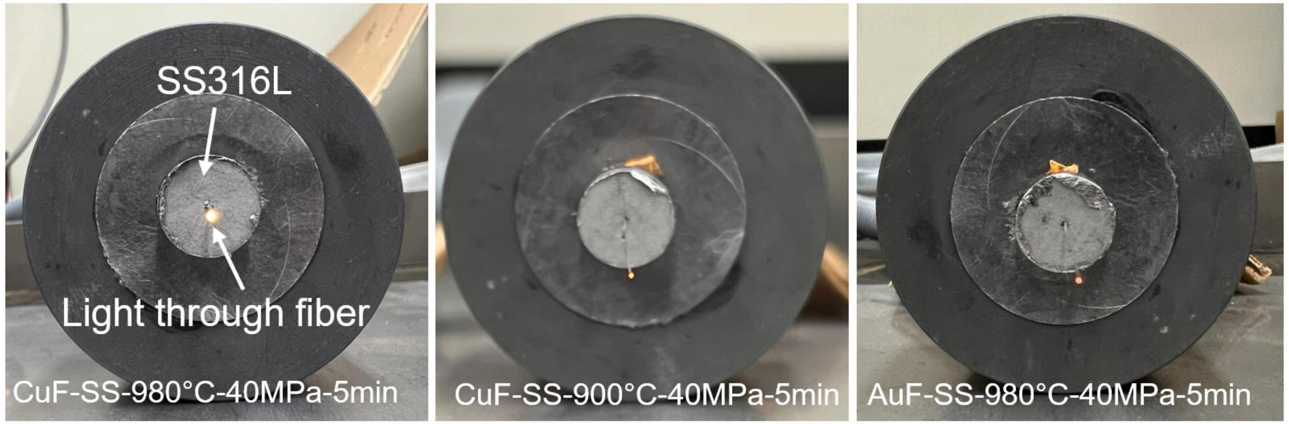

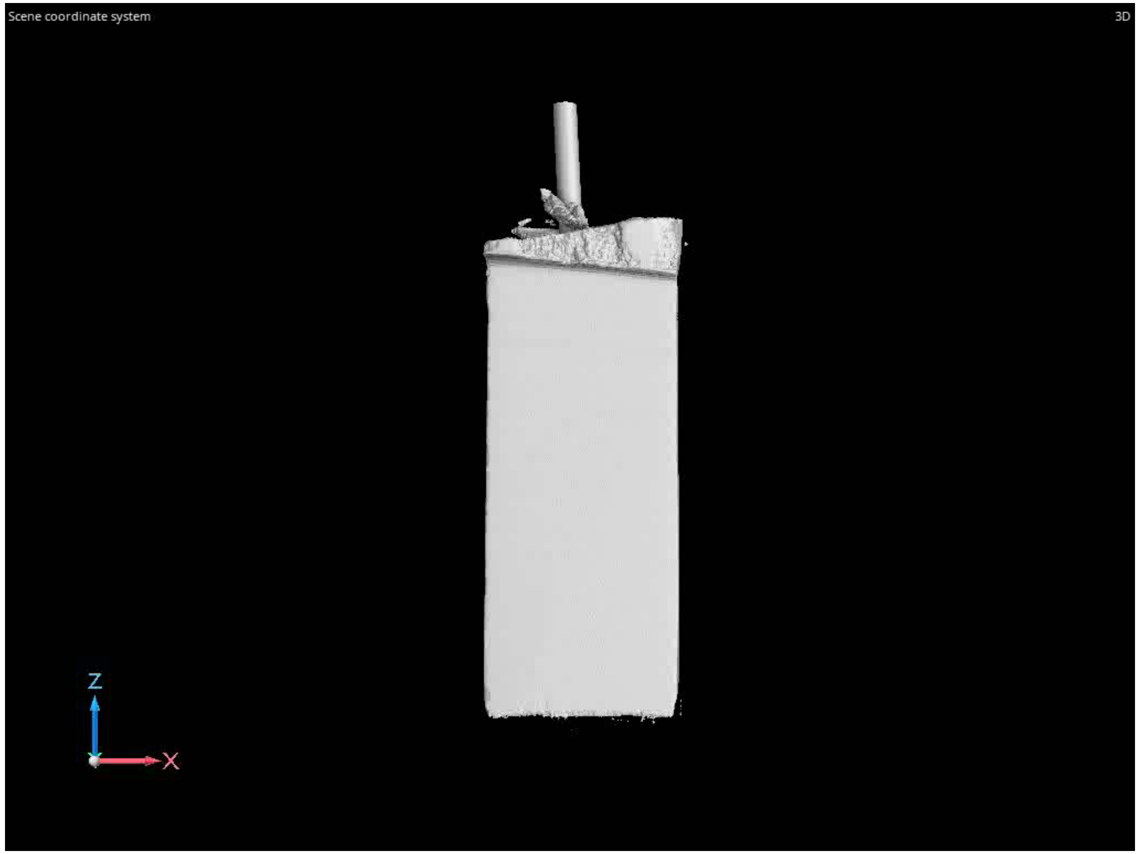

XCT scan of a sub volume of the sample with embedded fused silica optical fiber (CuF-SS-800-40-5).

4.3. Fiber-matrix bonding

- Embedded sapphire fiber
- Good overall fiber-matrix bonding quality with submicron-sized gaps observed at certain areas
- The cause of the gap was unclear (surface-only feature, fabrication due to CTE mismatch, delamination due to sample sectioning with the cutting saw)

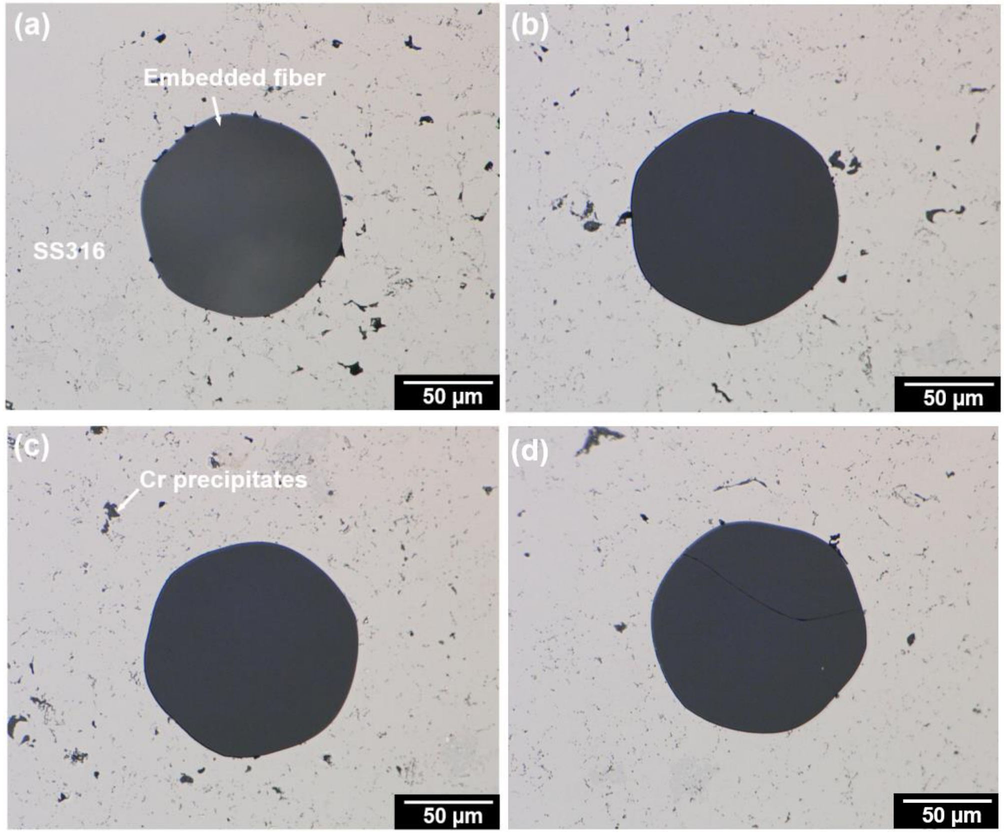

Optical microscope images showing cross-sections of fibers embedded at (a) 1000°C-50MPa-5min, (b) 1000°C-50MPa-10min, (c) 1050°C-50MPa-5min, and (d) 1100°C-50MPa-5min

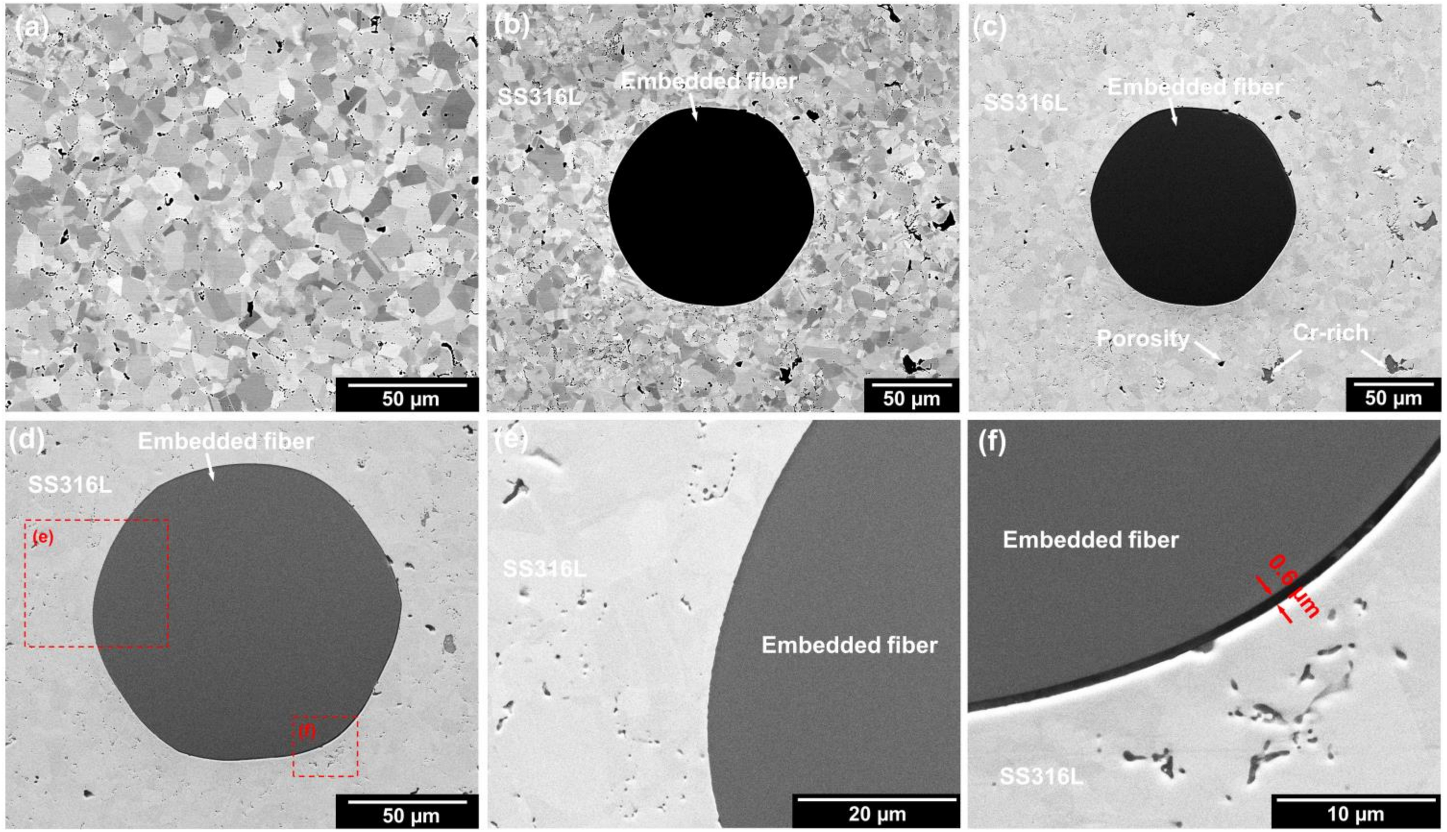

SEM micrographs showing features of the sample made at 1050°C-50MPa-5min. (a) Backscattered electron (BSE) micrograph of the matrix; (b) BSE and (c, d) secondary electron micrographs of the region adjacent to embedded fiber; (e) Magnified view of area e in (d); (f) Magnified view of area f in (d).

4.3. Fiber-matrix bonding

- Embedded sapphire fiber
- Elemental mapping indicated good fiber-matrix integration and fiber integrity
- Elemental diffusion (~2 µm) occurred at fiber-matrix interface (good fiber-matrix coupling)

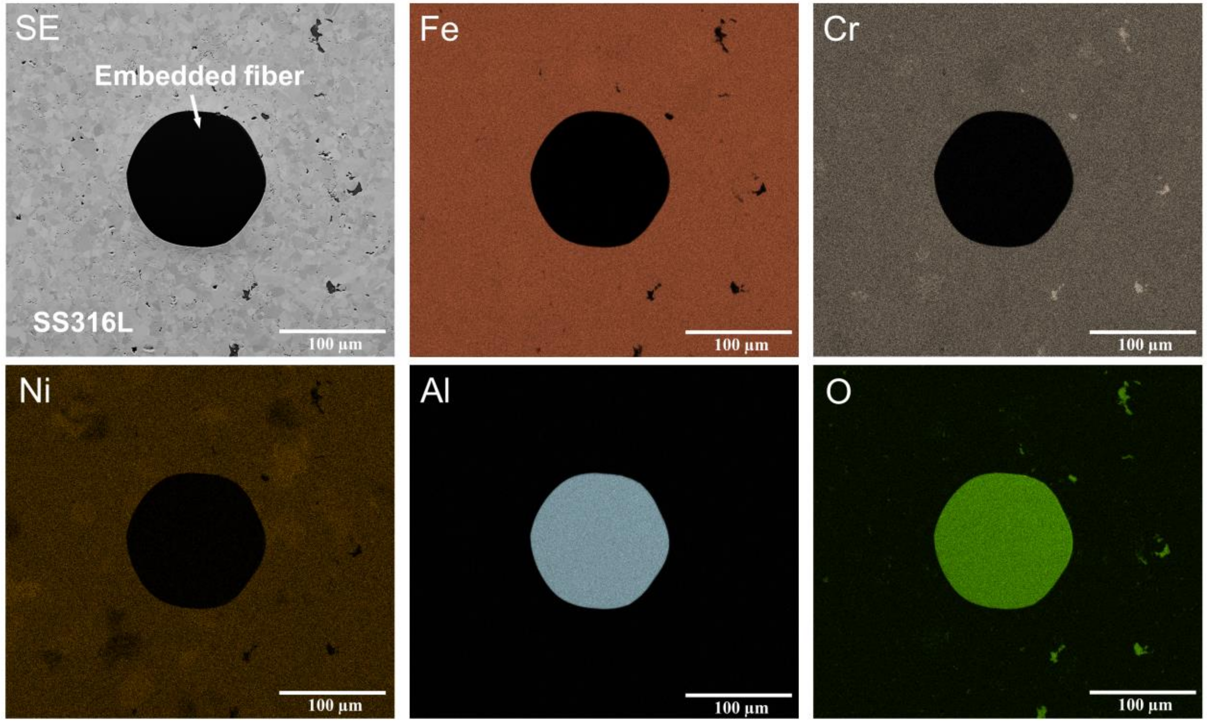

EDS maps of elemental distribution across the embedded fiber in the sample fabricated at 1050°C-50MPa-5min

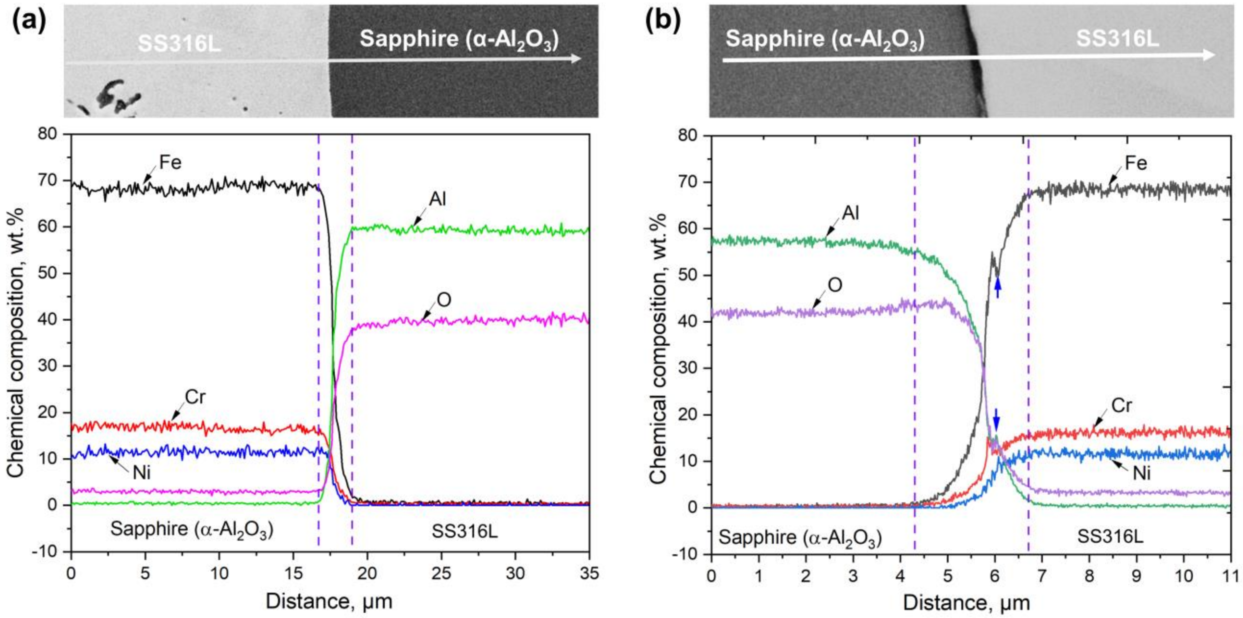

Elemental transition across the fiber-matrix interface in the sample fabricated at 1050°C-50MPa-5min. (a) EDS line scan from the matrix to sapphire across a well-bonded interface. (b) EDS line scan from sapphire to the matrix across an interface with a sub-micron gap.

4.3. Fiber-matrix bonding

- Embedded sapphire fiber
  - Increasing temperature, pressure and dwell time during EFAS contributed to better densification
  - Sample relative densities over 98% can be achieved at conditions greater than 1050°C-50MPa-5min
  - Refined grains in SS316L matrix. Embedded sapphire fiber features (0001) crystal orientation

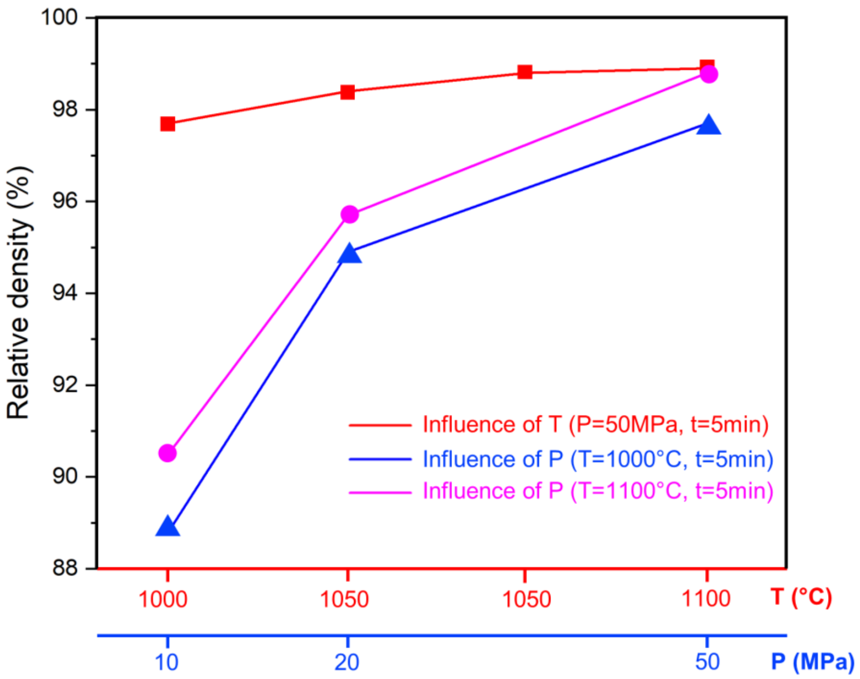

Effect of sintering temperature and pressure on the relative density of sintered samples.

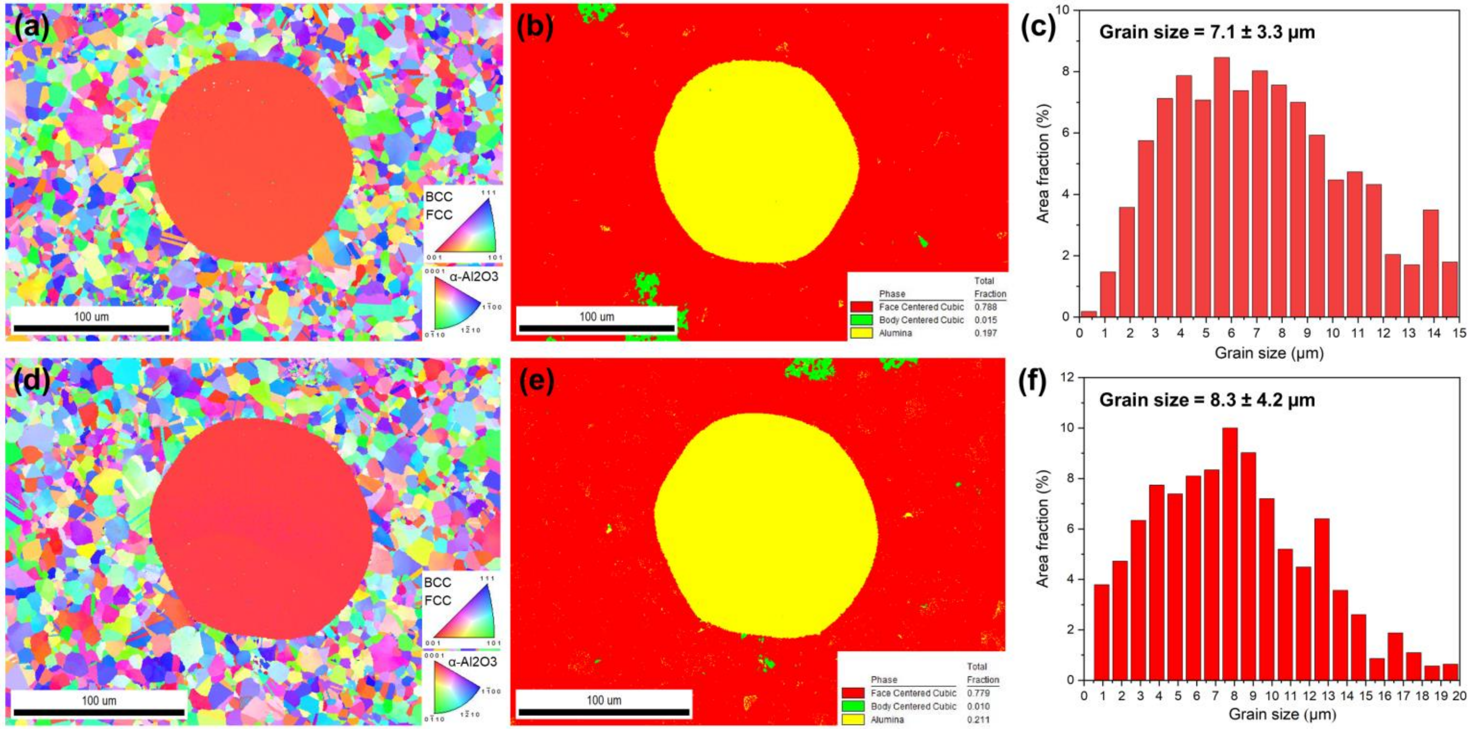

(a, d) EBSD grain orientation map, (b, e) phase map, and (c, f) grain size distribution on samples fabricated at (a-c) 1050°C-50MPa-5min and (d-f) 1050°C-50MPa-10min.

4.3. Fiber-matrix bonding

- <u>Embedded fused silica fiber (Cu-coated)</u>
- Safe EFAS parameter window for embedding fused silica fiber: 980°C (Cu- and Au-coated fiber). Higher temperature will melt the Cu-/Au-coatings.
- The density of SS316L increases with the increase of EFAS temperature, pressure and hold time.

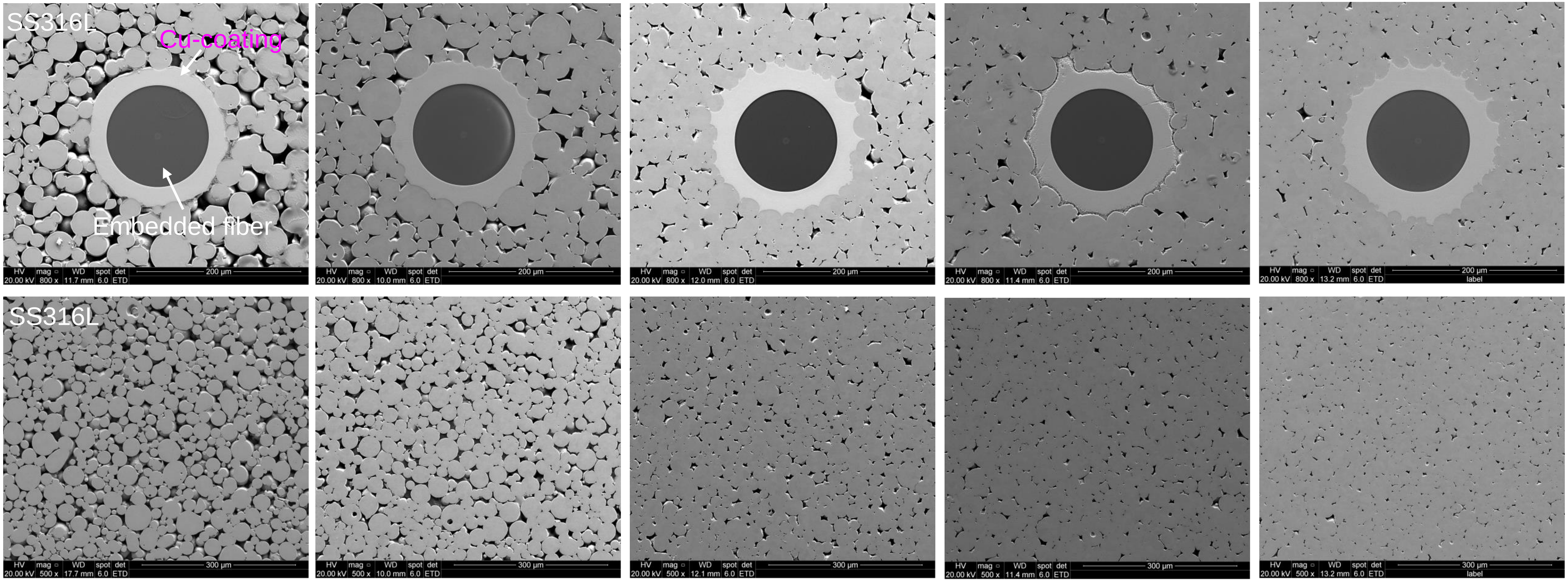

CuF-SS-800C-40MPa-5min | CuF-SS-900C-40MPa-5min | CuF-SS-980C-40MPa-5min | CuF-SS-980C-50MPa-5min | CuF-SS-980C-50MPa-10min

4.3. Fiber-matrix bonding

- Embedded fused silica fiber (Cu-coated)
- Elemental distribution across the bonding zone shows good bond between the fiber and matrix

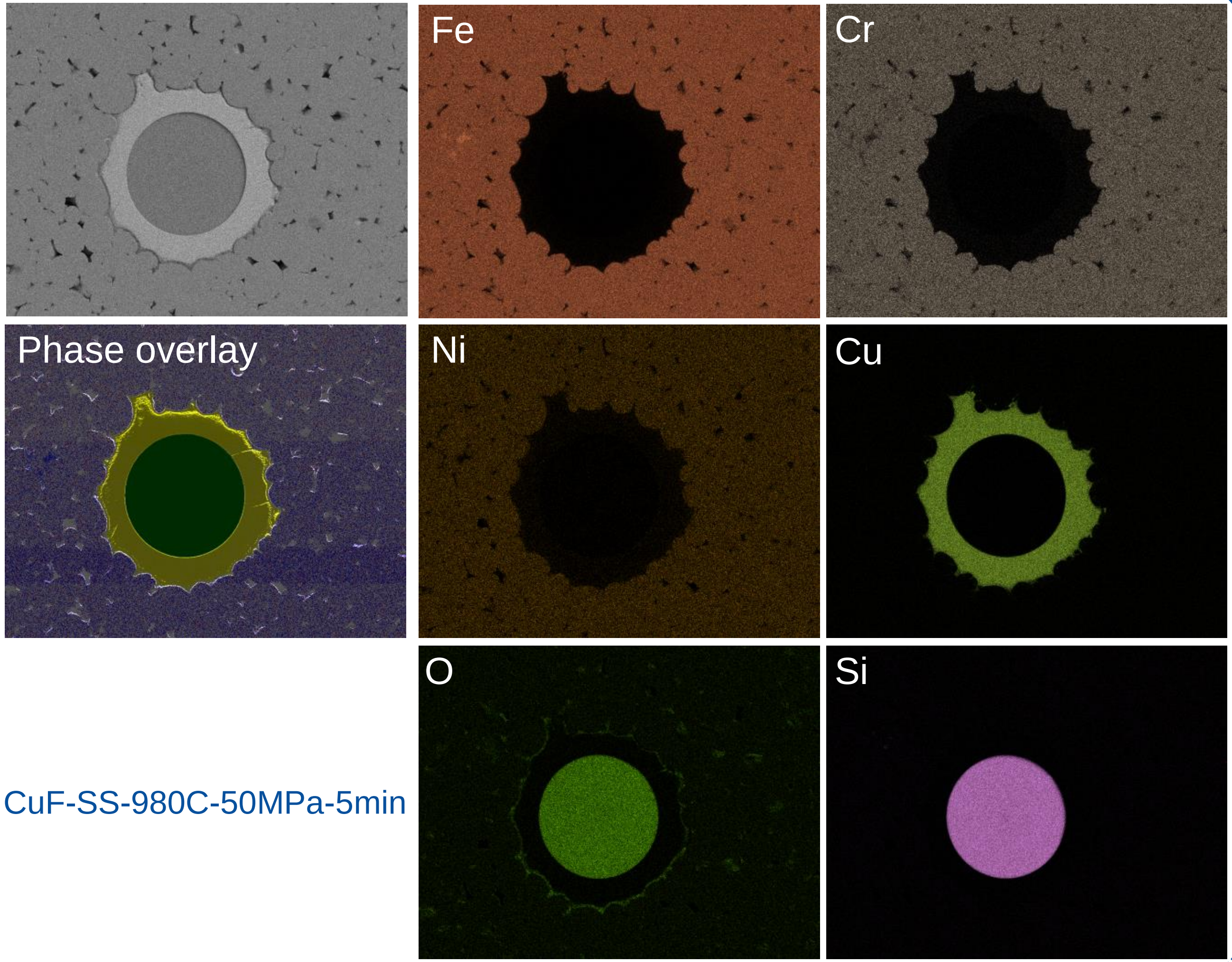

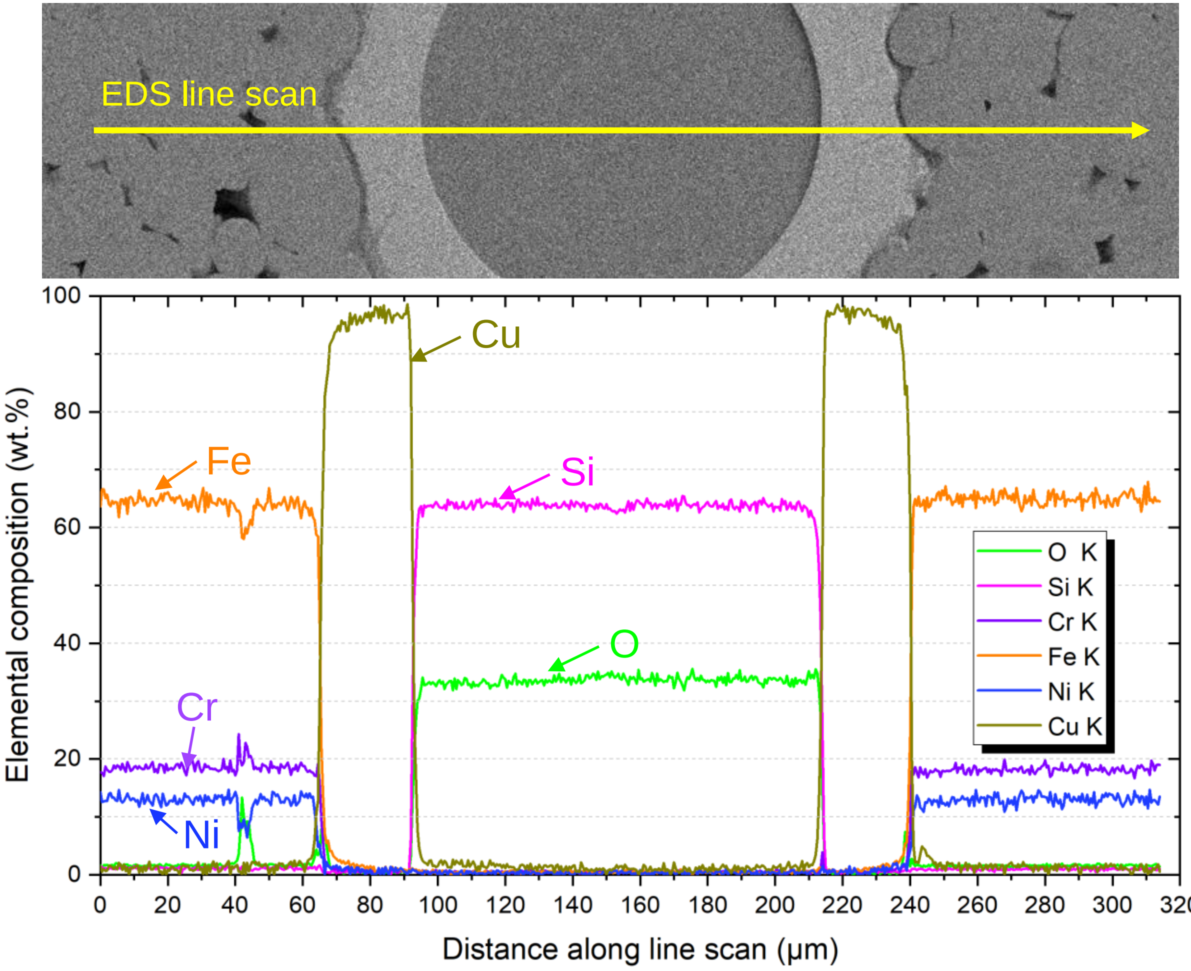

4.3. Fiber-matrix bonding

- Embedded fused silica fiber (Au-coated)
- Safe EFAS parameter window for embedding fused silica fiber: 980°C (Cu- and Au-coated fiber). Higher temperature will melt the Cu-/Au-coatings.
- The density of SS316L increases with the increase of EFAS temperature, pressure and hold time.

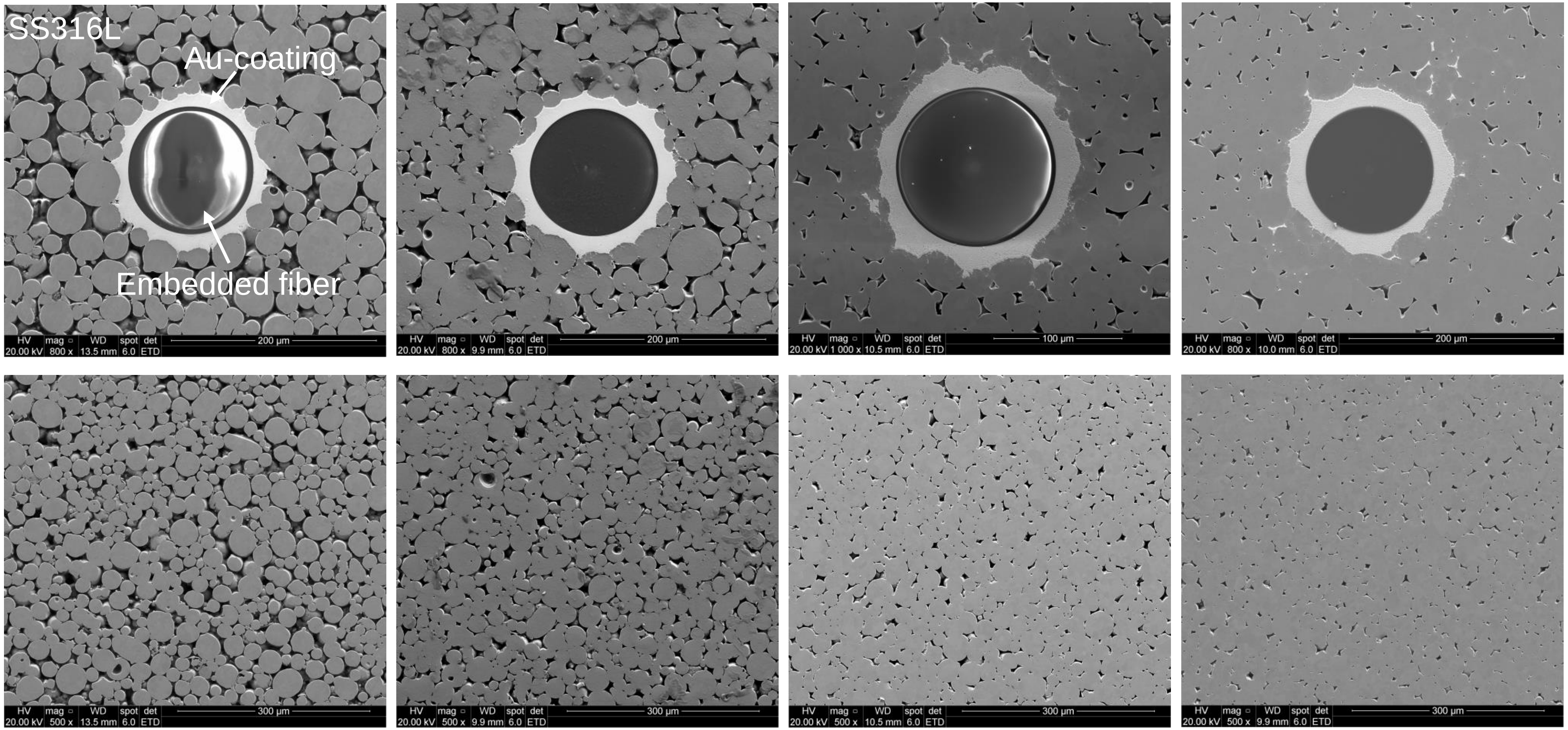

AuF-SS-800C-40MPa-5min | AuF-SS-900C-40MPa-5min | AuF-SS-980C-40MPa-5min | AuF-SS-980C-50MPa-5min

4.3. Fiber-matrix bonding

- Embedded fused silica fiber (Au-coated)
- Elemental distribution across the bonding zone shows good bond between the fiber and matrix

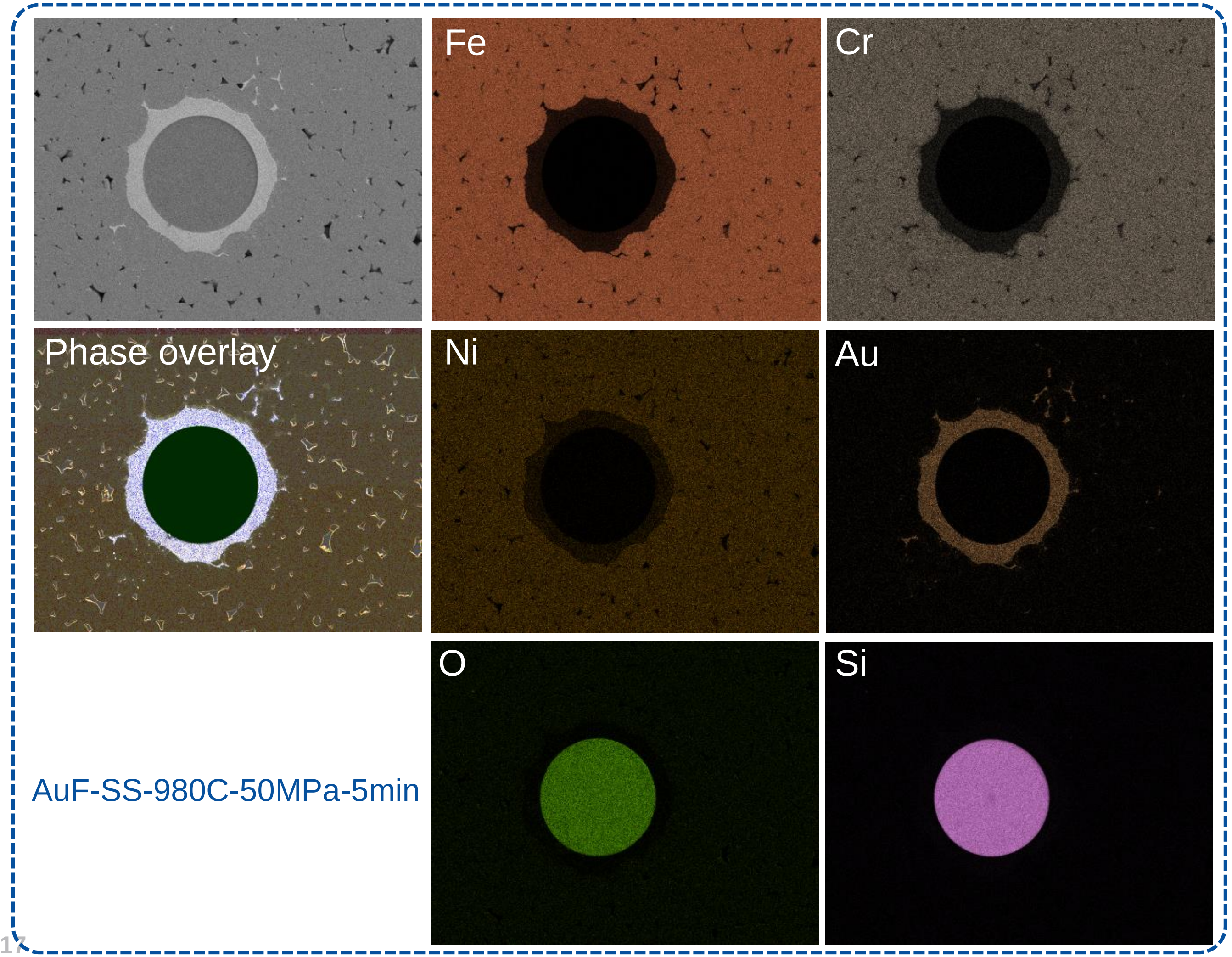

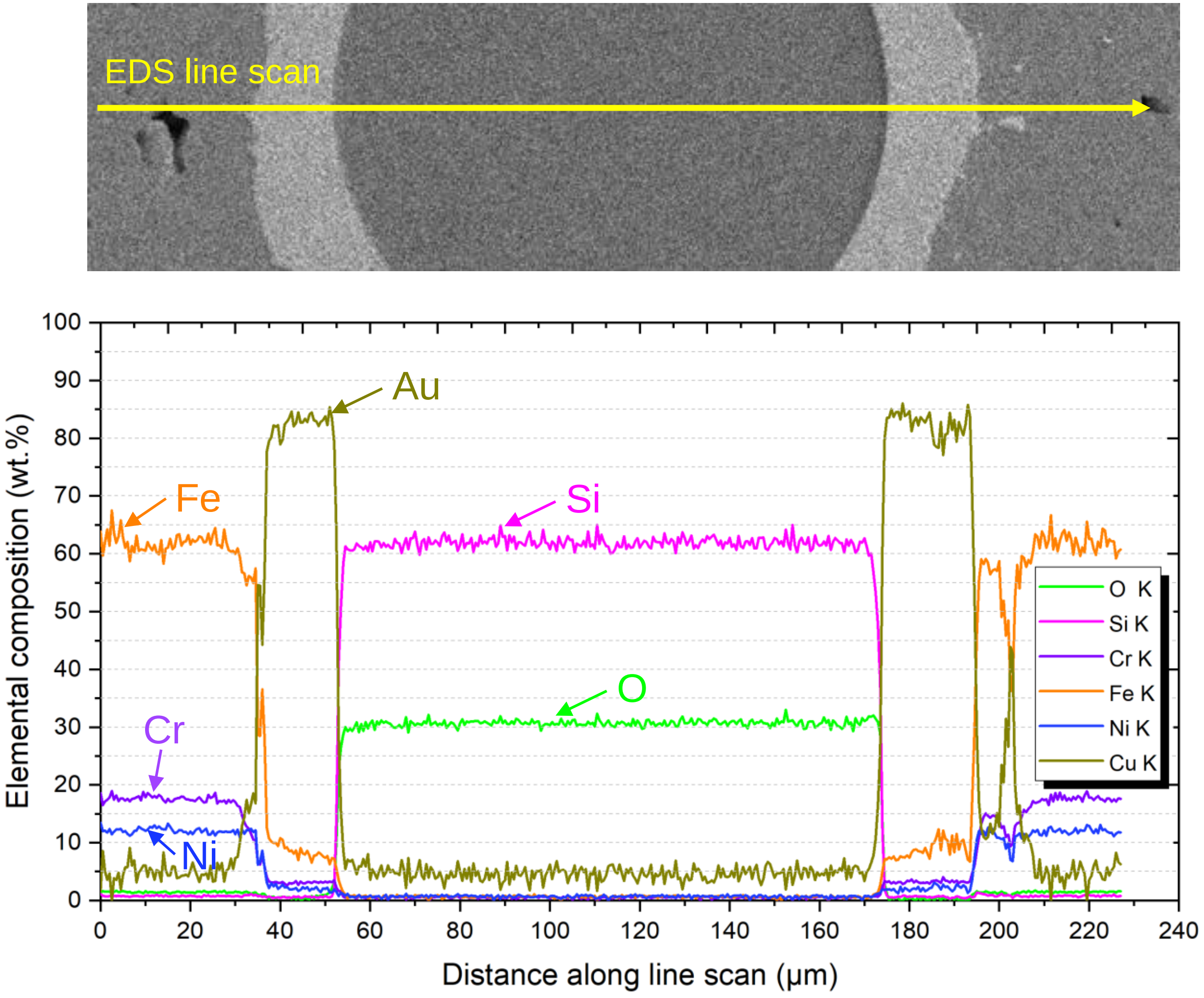

4.3. Fiber-matrix bonding

- Cu-coated fused silica fiber embedded in nickel
- Embedding fibers in nickel is easier due to the lower sintering temperatures (900°C) required to sinter nickel to achieve good density.

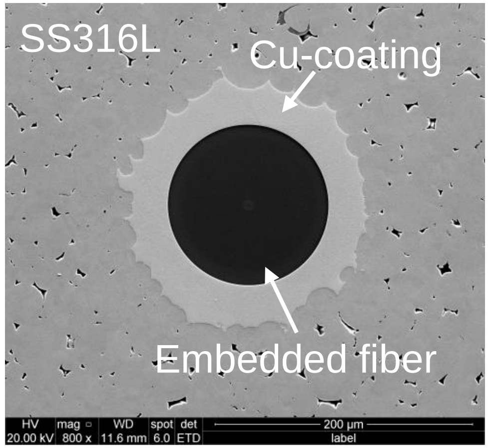

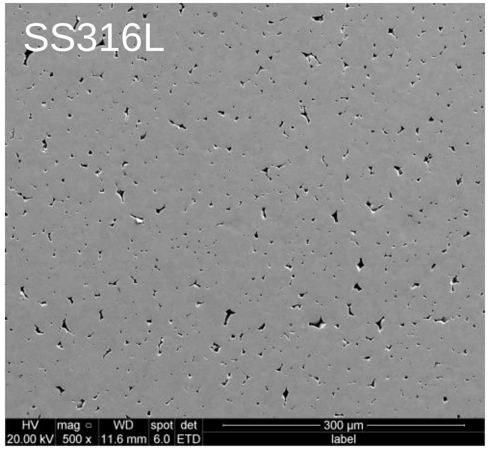

CuF-SS-980C-60MPa-10min

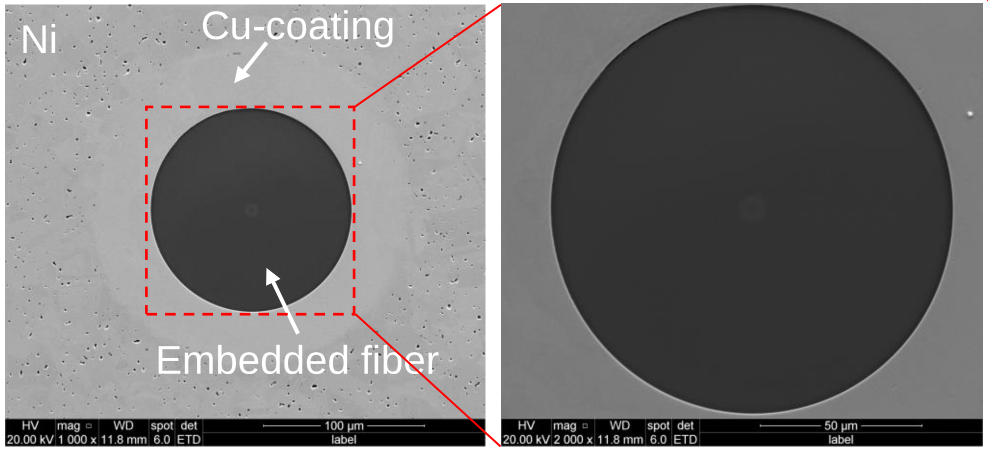

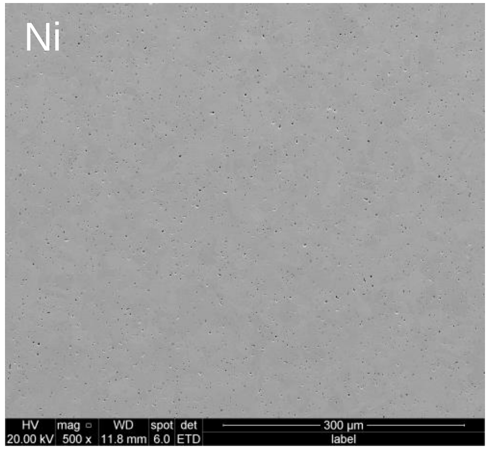

CuF-Ni-900C-50MPa-5min

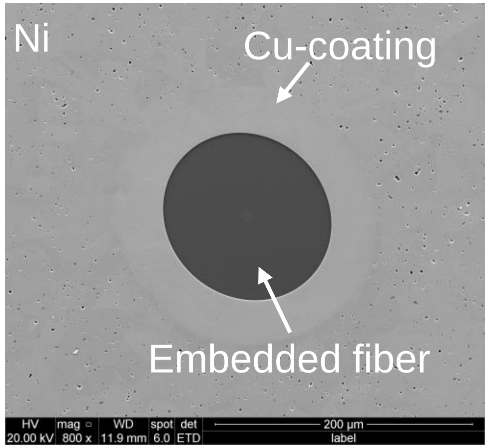

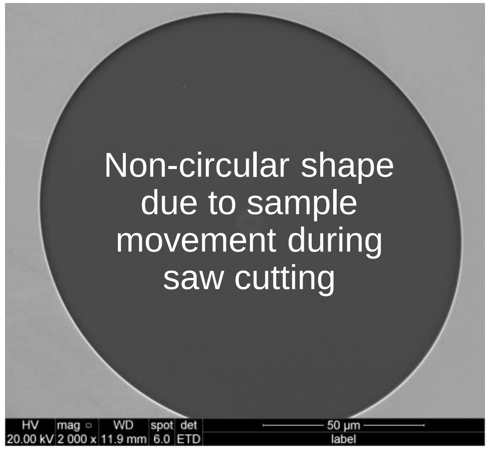

CuF-Ni-980C-50MPa-5min

4.3. Fiber-matrix bonding

- Cu-coated fused silica fiber embedded in nickel
- Elemental distribution across the bonding zone shows good bond between the fiber and matrix

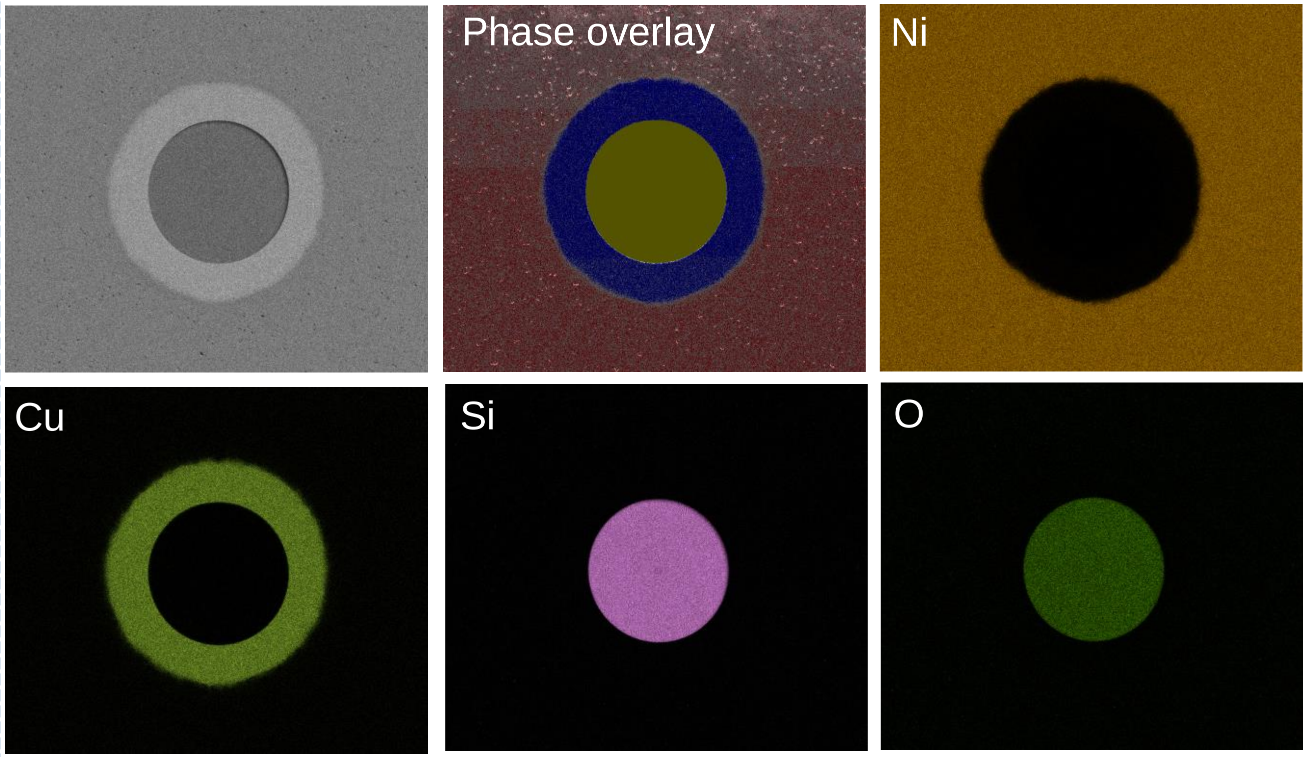

CuF-Ni-900C-50MPa-5min

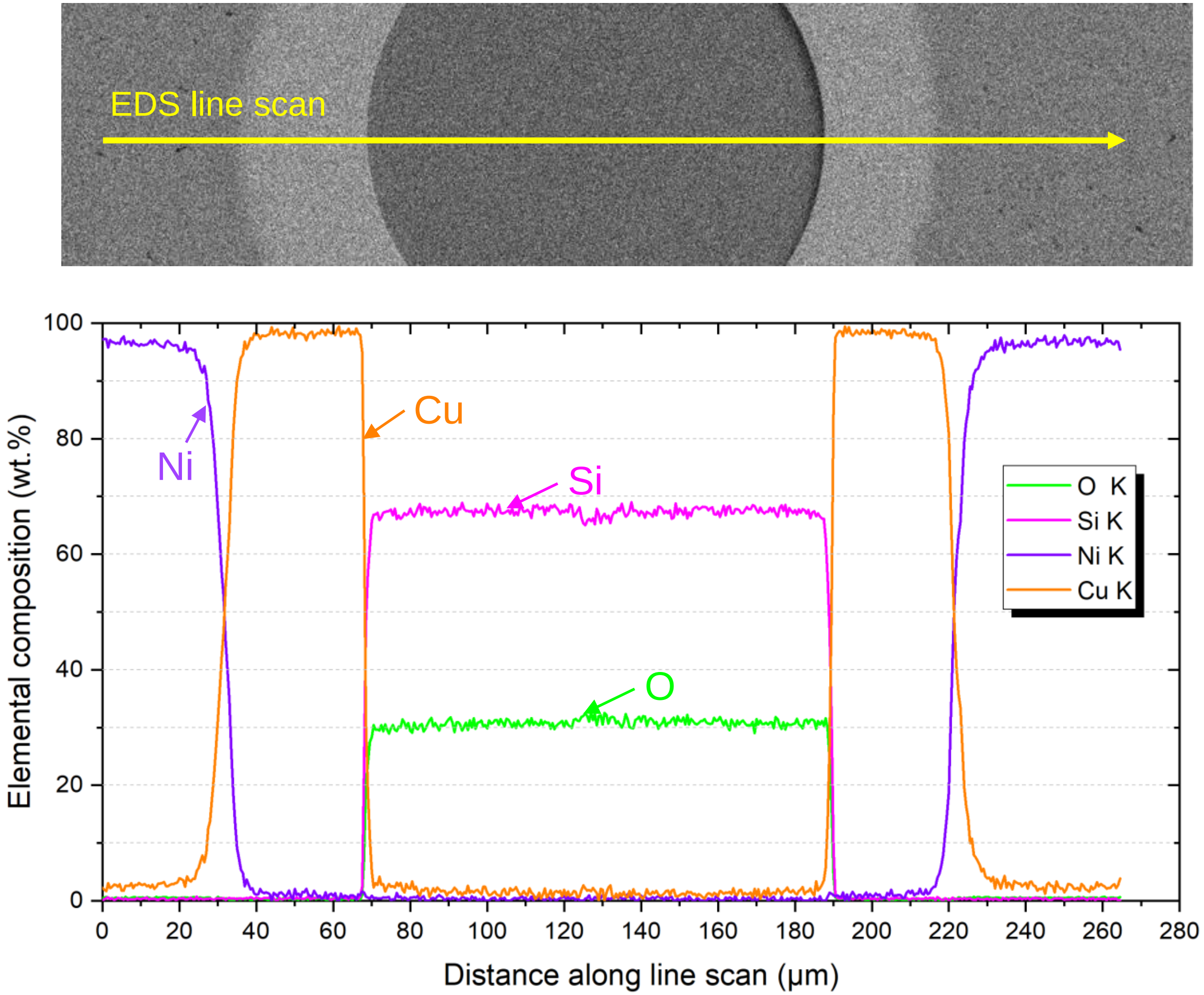

4.3. Fiber-matrix bonding

- Leak Test
- Low fabrication temperature resulted in interconnected pore network in the stainless-steel matrix and caused helium leak through the pore network
- SS with embedded fibers fabricated at 980℃ are leak tight
- Ni with embedded fibers are leak tight and have better sealing quality compared to SS due to better densification at lower temperatures

Leak test result on samples with embedded fused silica fibers using EFAS

	Sample ID.	Temperature (°C)	Pressure (MPa)	Dwell time (min)	Leak Test
Cu-coated fiber embedded in SS316L	CuF-SS-800-40-5	800	40	5	Leak around outer surface of sample (need better test setup)
	CuF-SS-900-40-5	900	40	5	Leak – due to pores at matrix grain boundaries (increase sintering parameters)
	CuF-SS-980-40-5	980	40	5	Leak around outer surface of sample (need better test setup)
	CuF-SS-980-50-5 (sample 1)	980	50	5	3.9×10^{-4}
	CuF-SS-980-50-5 (sample 2)	980	50	10	2.1×10^{-5}
	CuF-SS-980-60-10	980	60	10	-
Cu-coated fiber embedded in Ni	Ni only (reference)	900	40	5	3.2×10^{-7}
	CuF-Ni-900-50-5	900	50	5	1.7×10^{-7}
	CuF-Ni-980-50-5	980	50	5	-

4.4. Functionality of Embedded Fiber

- Embedded sapphire fiber
- Optical attenuation: optical attenuation due to fiber encapsulation was observed and the attenuation was affected by fabrication parameters

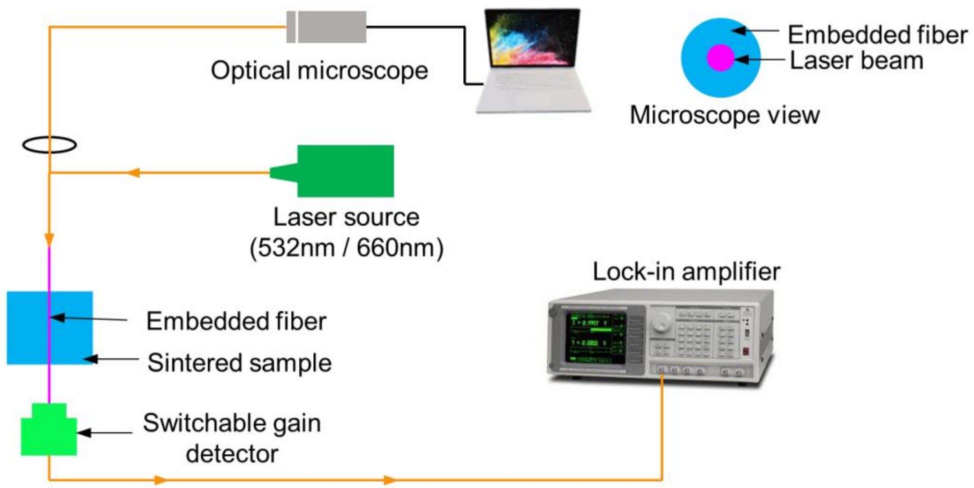

Optical attenuation of the fibers before and after encapsulation at different laser wavelengths relative to the input laser power and the as-received fiber

Laser wavelength	As-received	Sample #2 (1000°C-20MPa-5min)	Sample #5 (1050°C-50MPa-5min)	Sample #9 (1100°C-50MPa-5min)
Relative to input signal power (dB)				
532 nm	1.57	1.87	3.02	3.31
660 nm	1.43	1.97	2.71	3.29
Relative to as-received fiber (dB)				
532 nm	-	0.30	1.45	1.74
660 nm	-	0.54	1.28	1.86

4.4. Functionality of Embedded Fiber

- Embedded fused silica fiber

- Cu-coated fibers were OBR scanned before embedding using EFAS
- Pre-embedding OBR scans indicate that the last ~1.5'' of coated section of fiber should be avoided for EFAS embedding experiments for accurate readings

Pre-embedding OBR scanned fibers

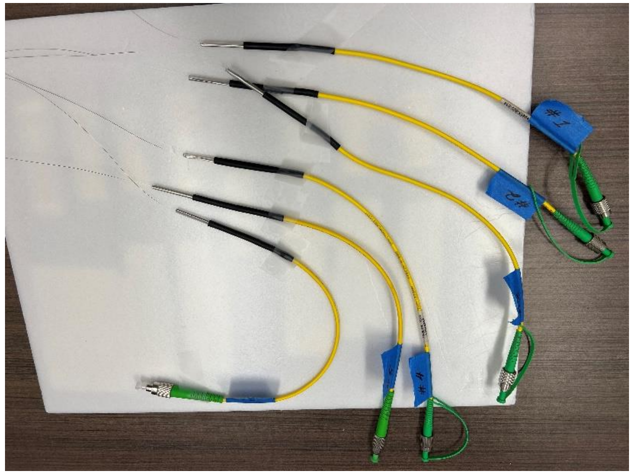

Fiber #1

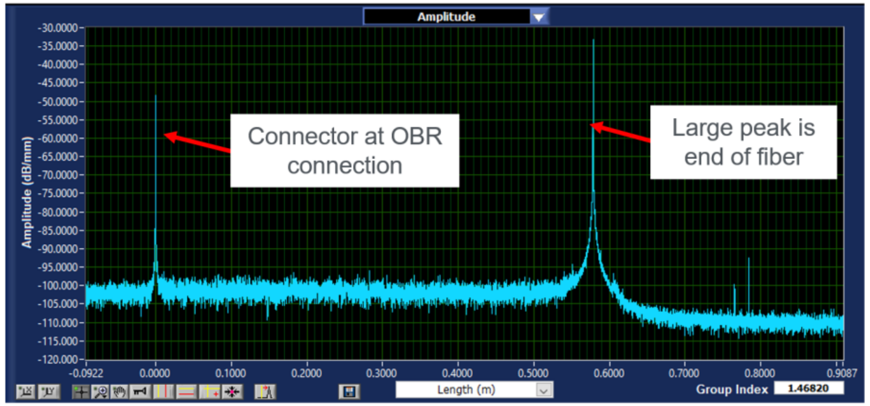

Fiber #2

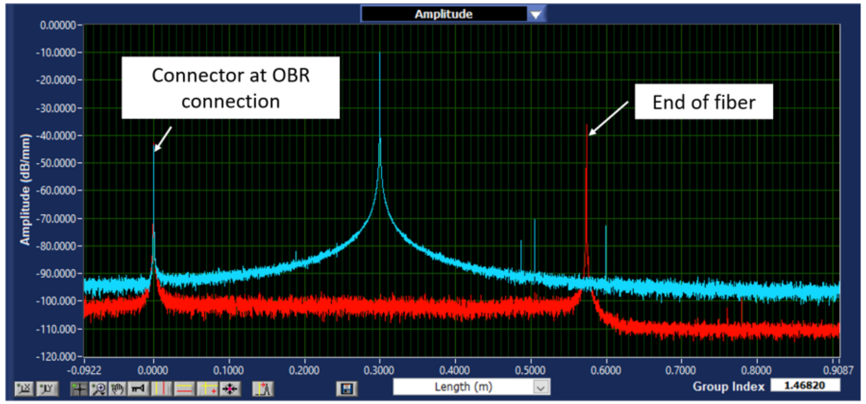

Fiber #3

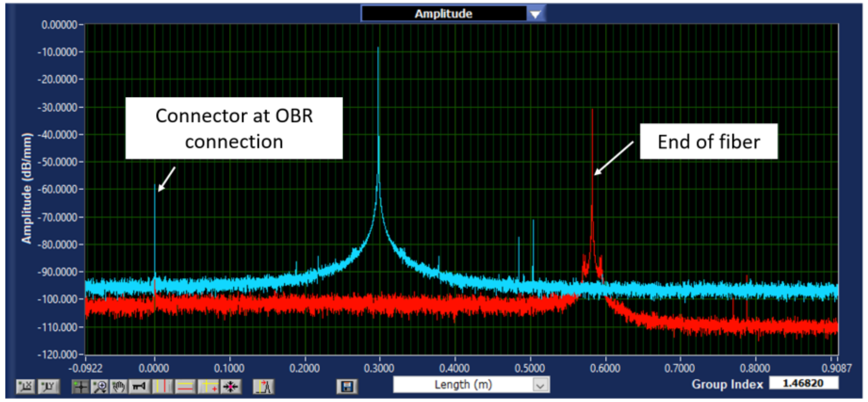

Fiber #4

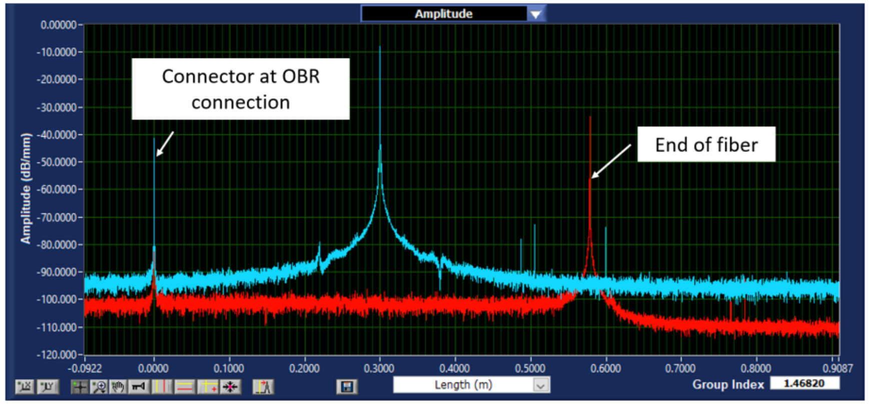

4.4. Functionality of Embedded Fiber

- Embedded fused silica fiber
- Embedding experiments and OBR scan test setup

Embedded fibers via EFAS

#1: Embedded in SS at 950°C-40MPa-5min

#2: Embedded in SS at 900°C-40MPa-5min

#3: Embedded in Ni at 900°C-40MPa-5min

#4: Embedded in Ni at 800°C-40MPa-5min

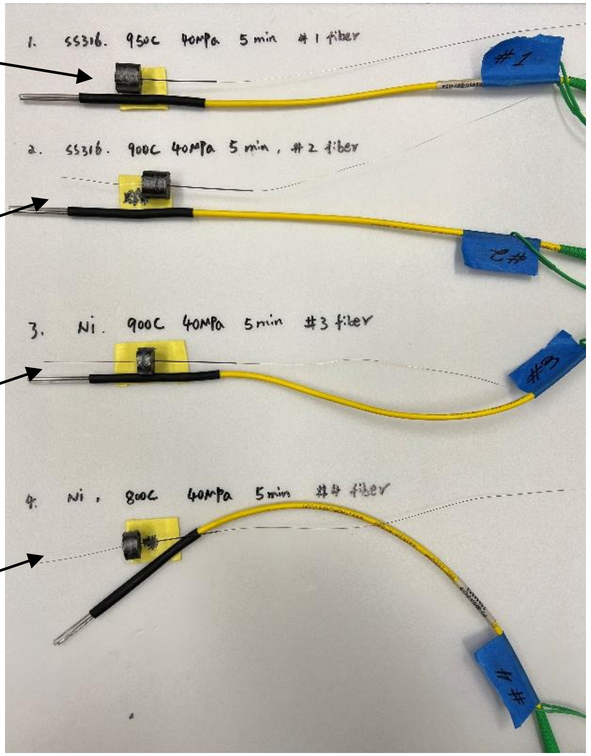

Post-embedding OBR scan on fiber #3 (embedded in Ni at 900°C)

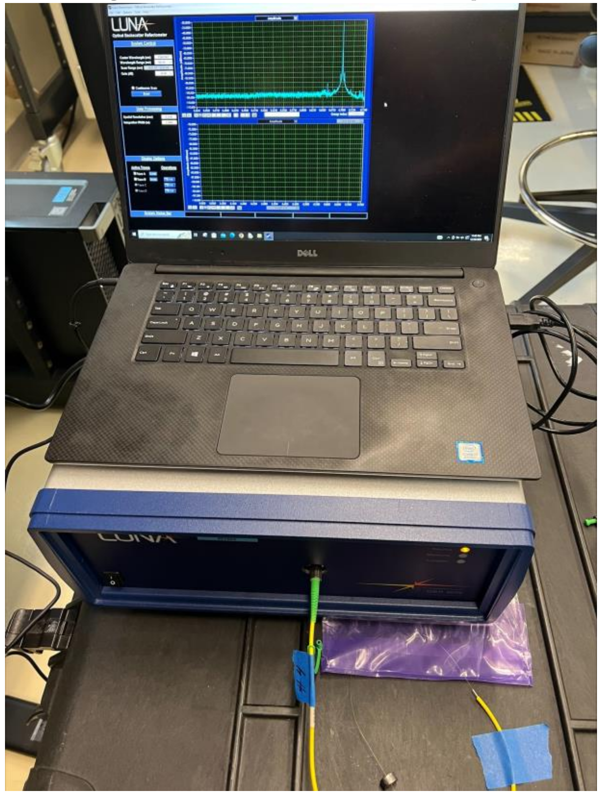

4.4. Functionality of Embedded Fiber

- Embedded fused silica fiber

- Insertion loss from the EFAS-fabricated Nickel block is -0.43~-0.52 dB (similar to a clean fiber connector). Increasing fabricating conditions caused more insertion loss.
- Mechanical stress is suspected to cause the insertion loss and return loss. Thermal heating (stress relief) on embedded fiber may benefit return loss

Overview

Post-embedding OBR scan on fiber #3 (Ni at 900°C)

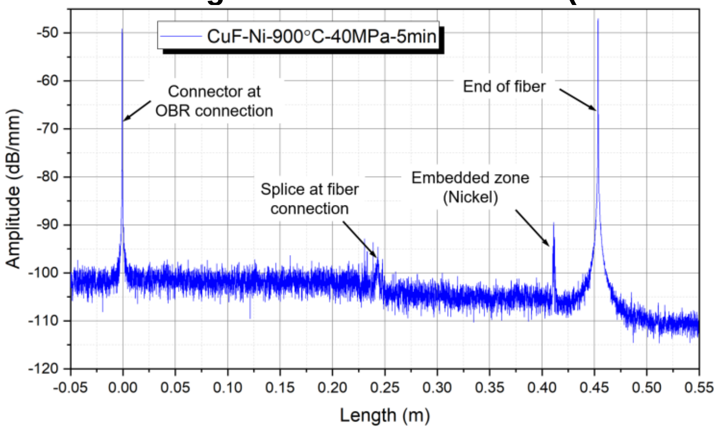

Post-embedding OBR scan on fiber #4 (Ni at 800°C)

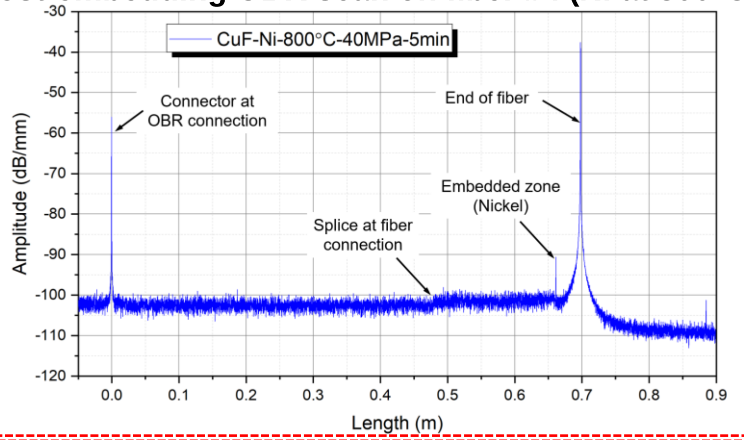

Enlarged view of embedded zone

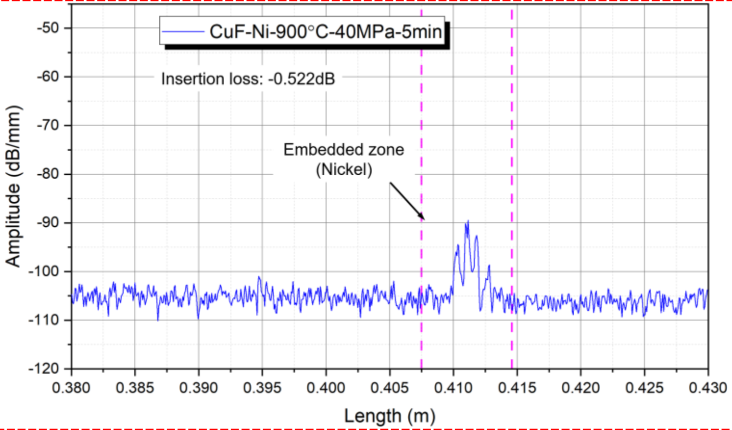

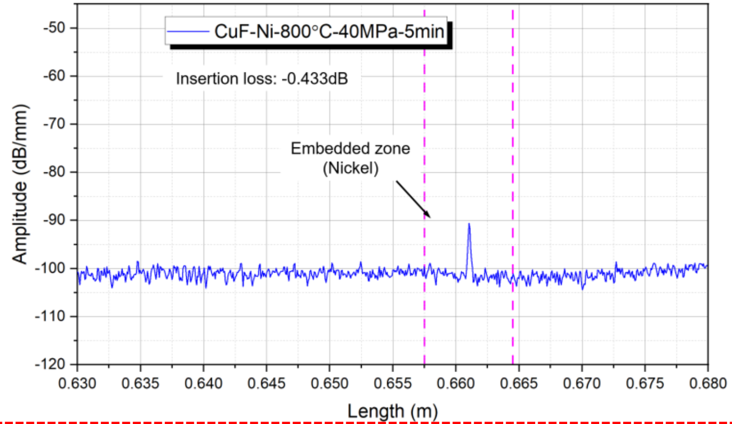

Sample ID	Insertion Loss	Return Loss
CuF Ni-900-40-5	-0.52 dB	-9.75 dB
Cu-F Ni-800-40-5	-0.43 dB	-10.8 dB

No losses outside of the fiber, indicating the return loss is solely a result of a Fresnel reflection resulting from a strain at the embedding site

$$RL = -10\log(P_{ST}) = -10\log\left(\frac{P_0 - P_B}{P_1 - P_B}(P_2 - P_B) - (P_0 - P_B)/2\right).$$

Kregel, et al. Return loss measurement in the presence of variable insertion loss using optical frequency domain reflectometry, 2006.

4.4. Functionality of Embedded Fiber

- Embedded fused silica fiber
- Insertion loss and return loss from the EFAS-fabricated stainless-steel blocks is challenging to quantify, due to missing fiber sections at the end of the fiber (breaks during handling)

Post-embedding OBR scan on fiber #1 (SS at 950°C)

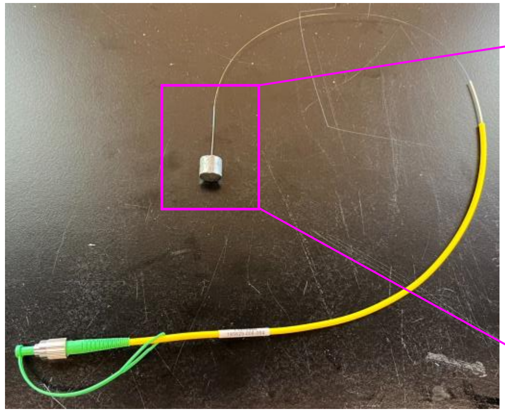

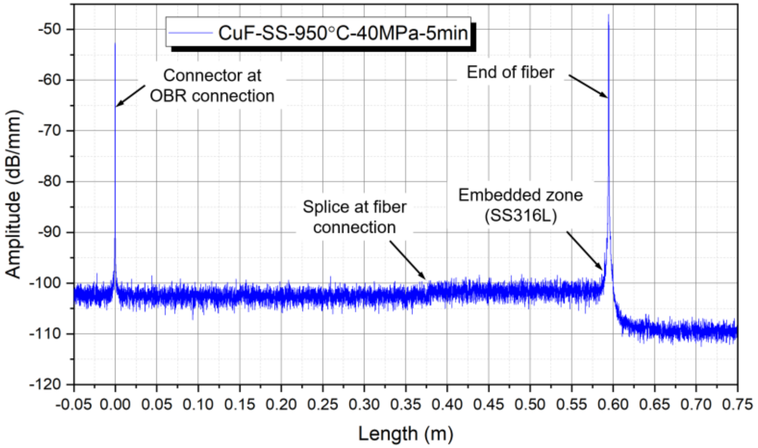

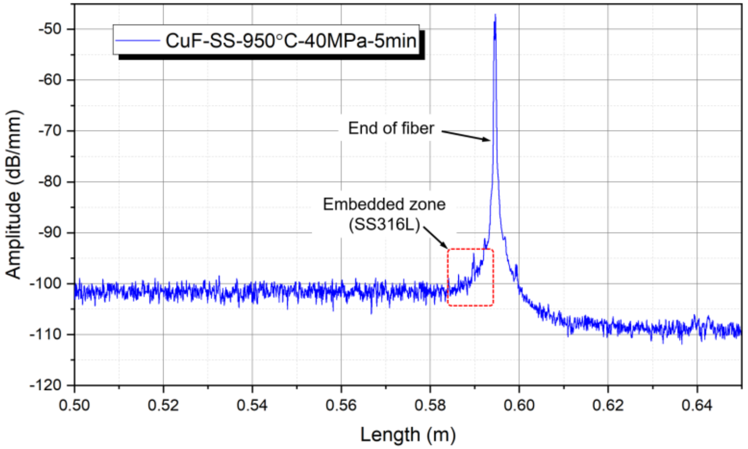

Post-embedding OBR scan on fiber #2 (SS at 900°C)

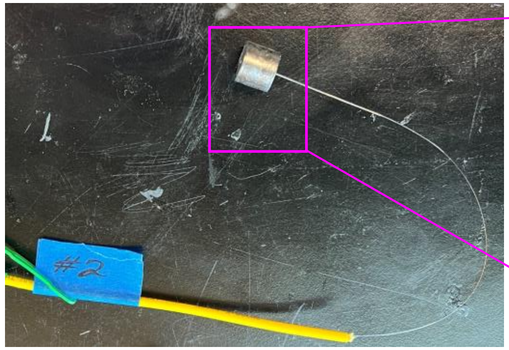

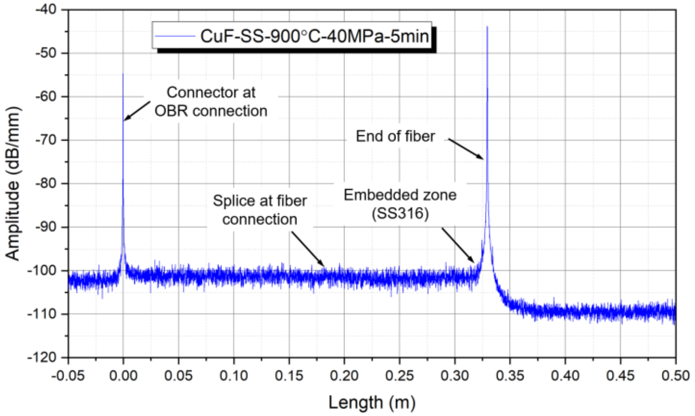

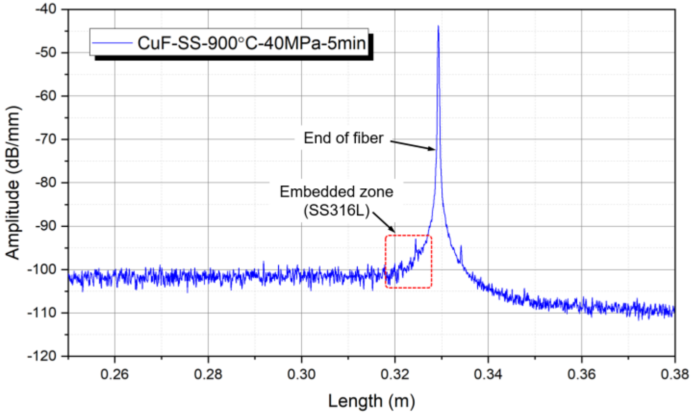

4.5. Mechanical Properties

- Embedded sapphire fiber
- Superior tensile strength of the as-fabricated matrix much higher than those of the ASTM wrought standard and SS316L fabricated by other advanced manufacturing techniques
- Materials with embedded fibers exhibited limited reduction in tensile strength

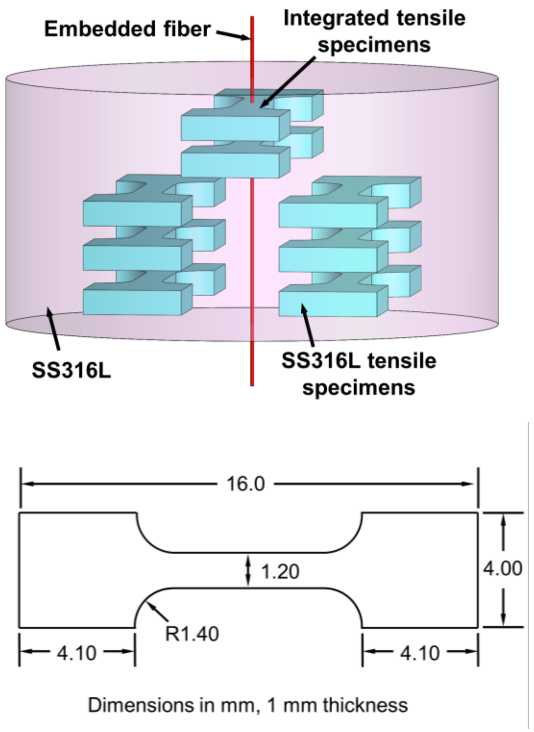

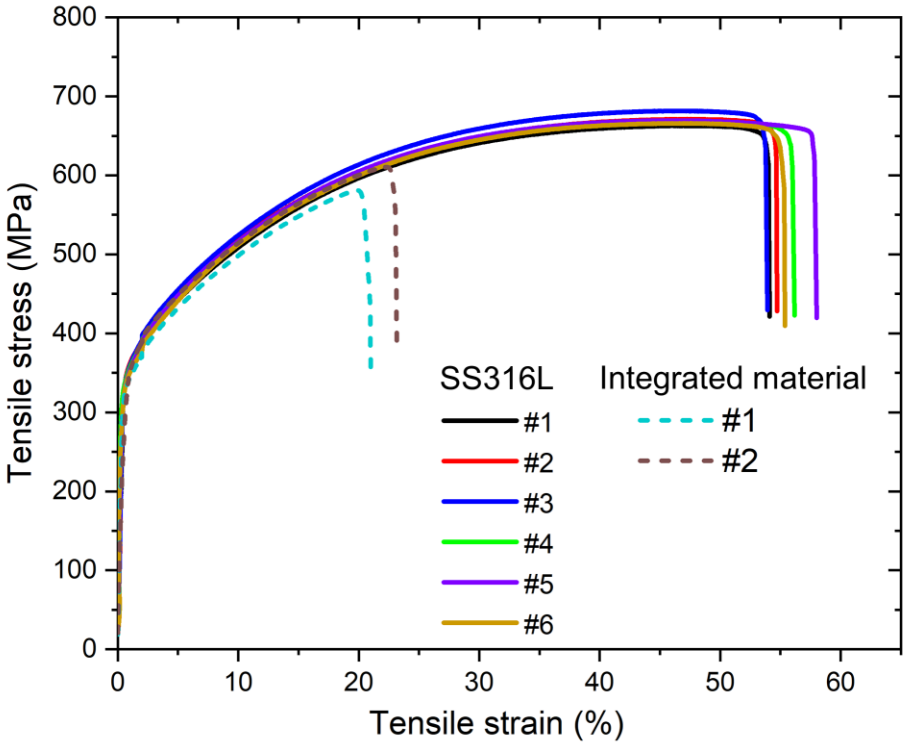

Tensile stress-strain curves obtained from the sintered matrix and matrix with integrated fiber (sample fabricated at 1050°C-50MPa-5min).

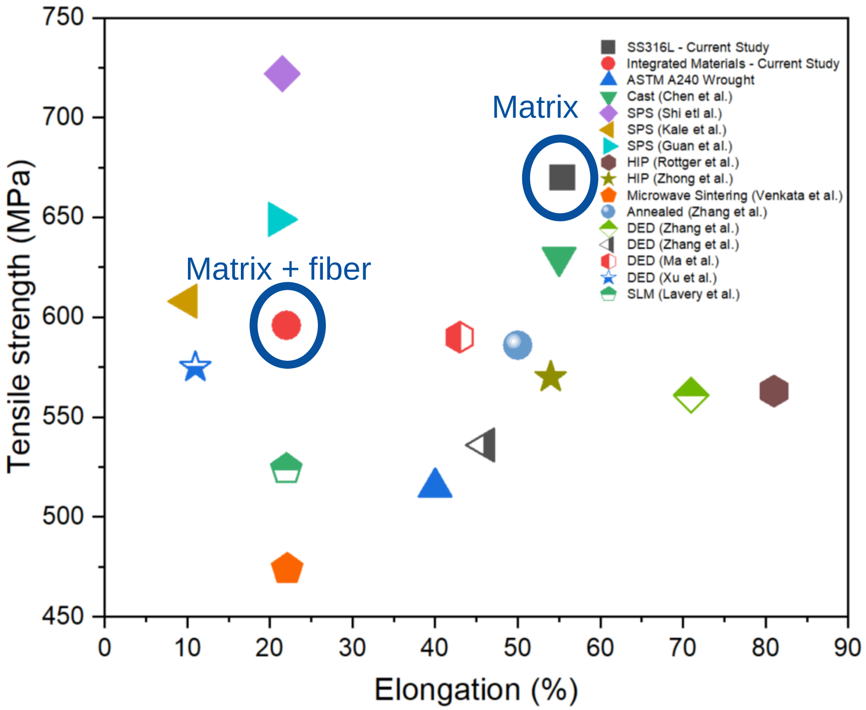

Results of tensile properties of the as-fabricated matrix and integrated materials as well as the comparison of obtained data with the literature

4.6. Machinability

- Embedded fused silica fiber in SS316L and nickel
- Demonstrated machinability of the samples for optical fiber feedthrough applications.
- Leak tests were conducted on the machined samples.

As-fabricated (before machining)

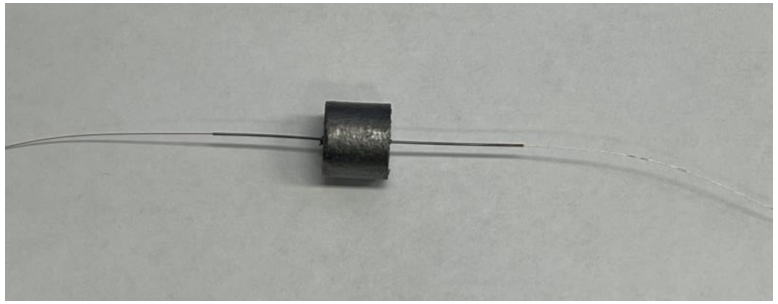

Post machining

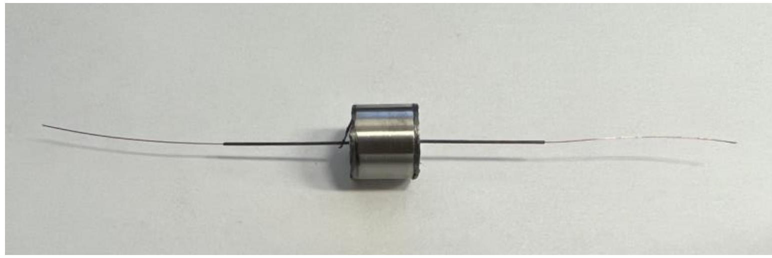

Examples of machined samples with embedded fibers

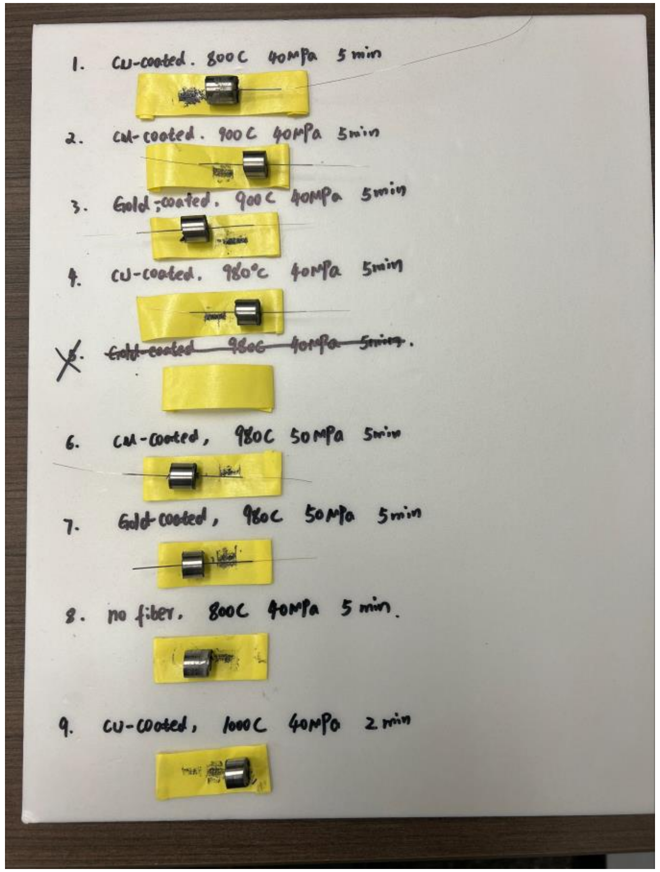

4.7. Fiber properties after thermal cycling

- SS and nickel samples (half sample) with embedded fibers experienced 50 cycles thermal treatment from 500°C to 700°C in a tube furnace in air

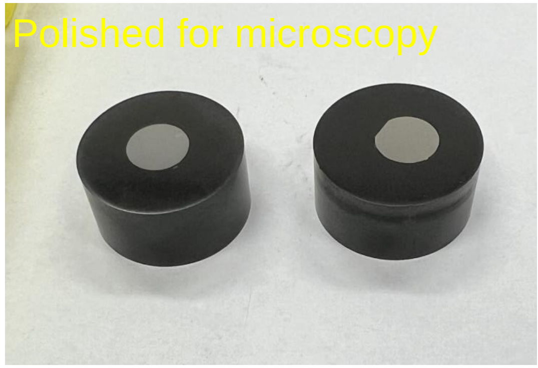

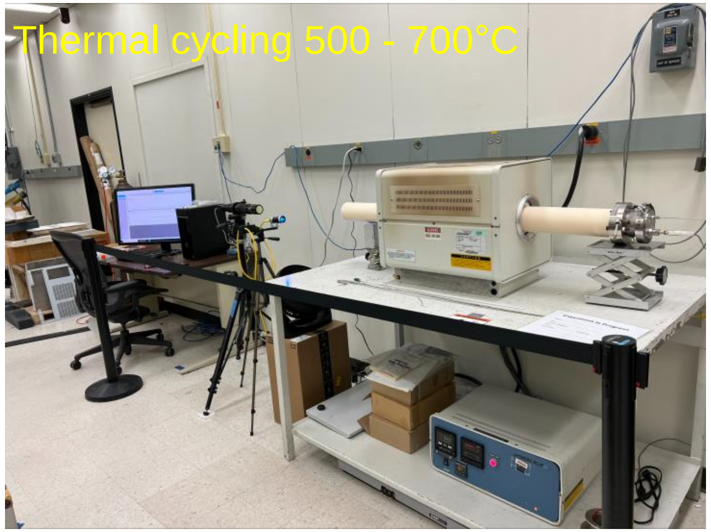

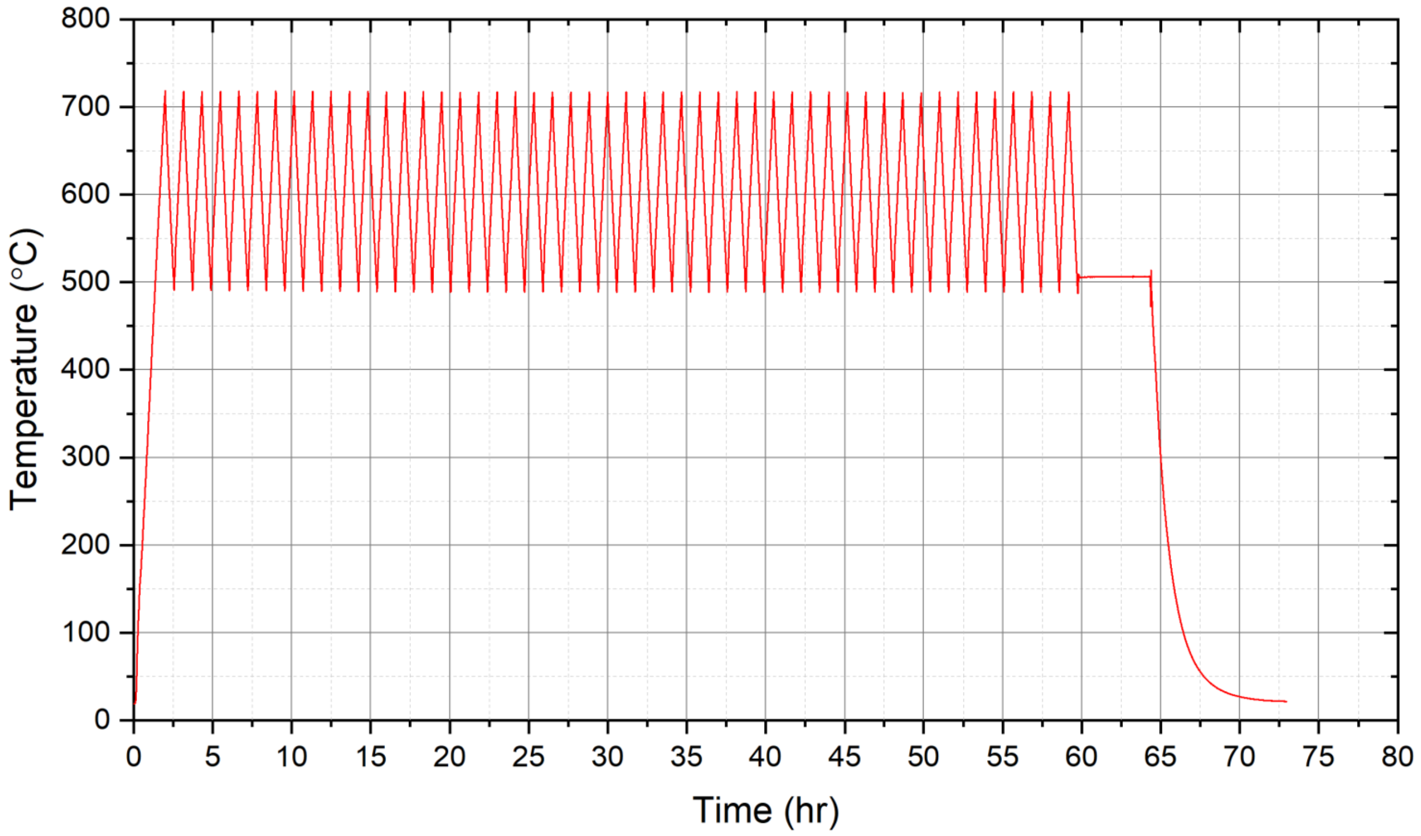

4.7. Fiber properties after thermal cycling

- Embedded fused silica fiber in SS316L (fabricated at 980°C-40MPa-5min)
- Fiber is intact after 50 cycles thermal treatment from 500°C to 700°C
- Cr-rich oxide layer was formed between SS and embedded fiber, due to reaction of diffused Cr with oxygen
- Whole sample should be heat treated, cut in half to reveal the cross-section, and inspected

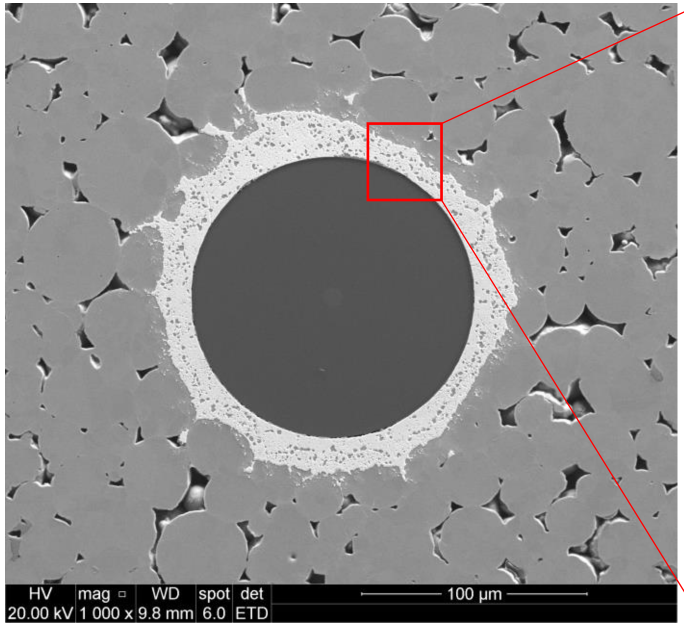

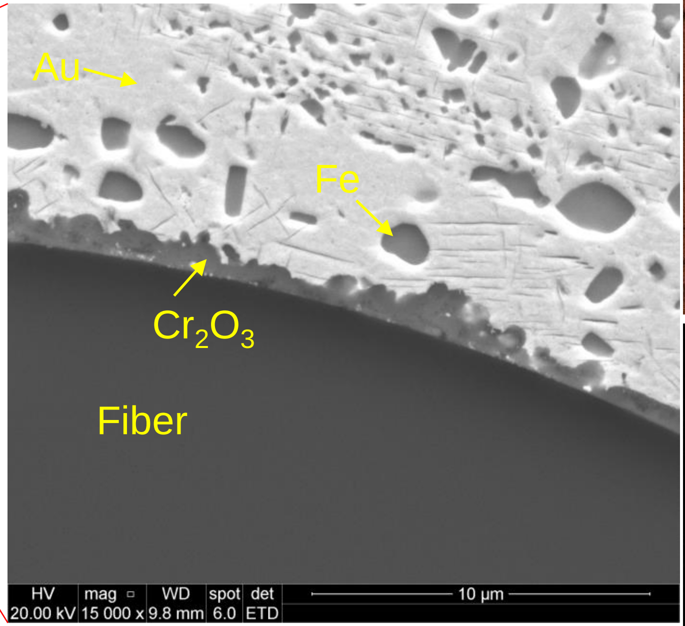

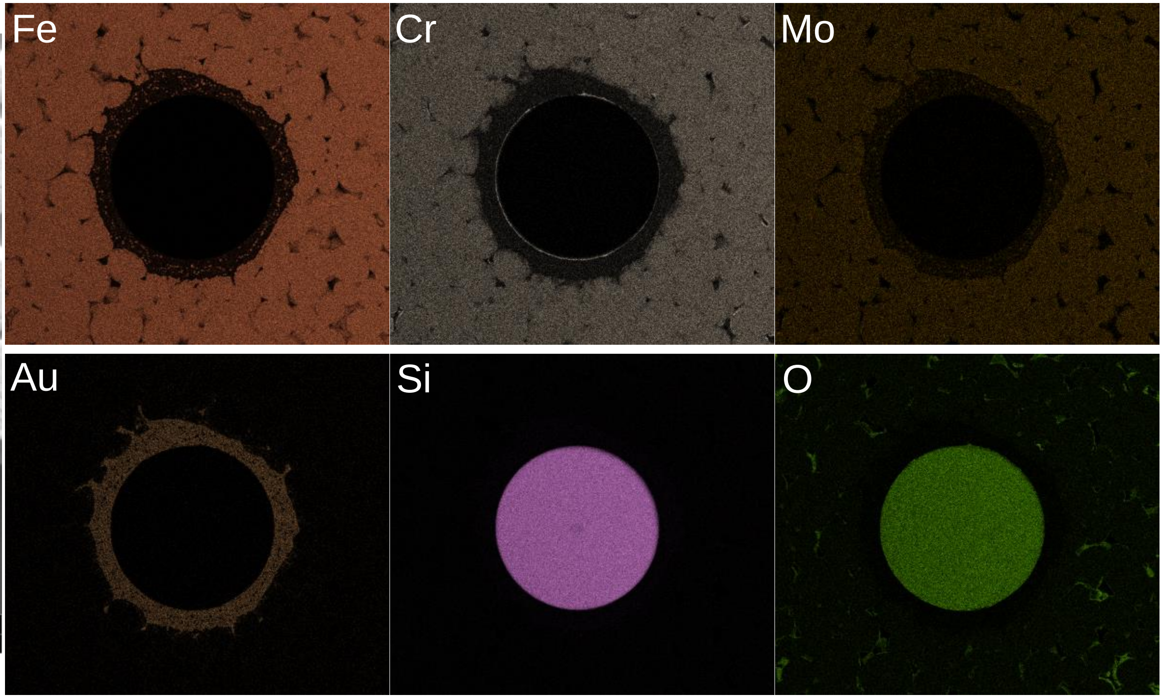

4.7. Fiber properties after thermal cycling

- Embedded fused silica fiber in Nickel (fabricated at 980°C-40MPa-5min)
- Fiber is intact after 50 cycles thermal treatment from 500°C to 700°C
- No obvious change of fiber-matrix bonding and elemental distribution after thermal cycling

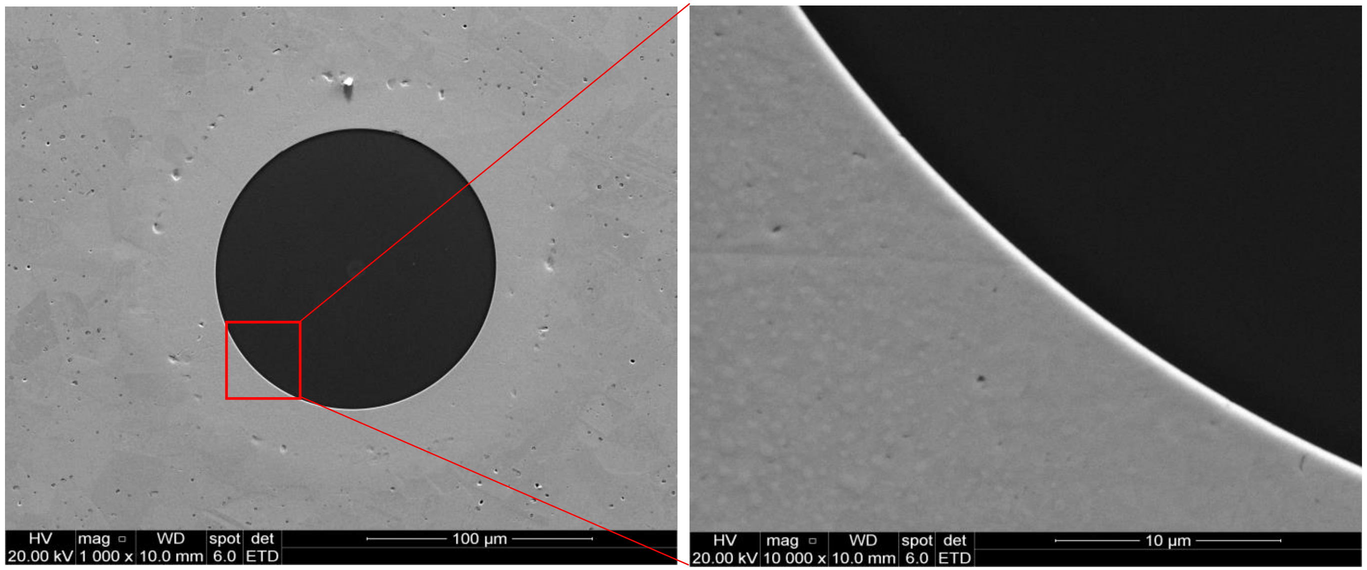

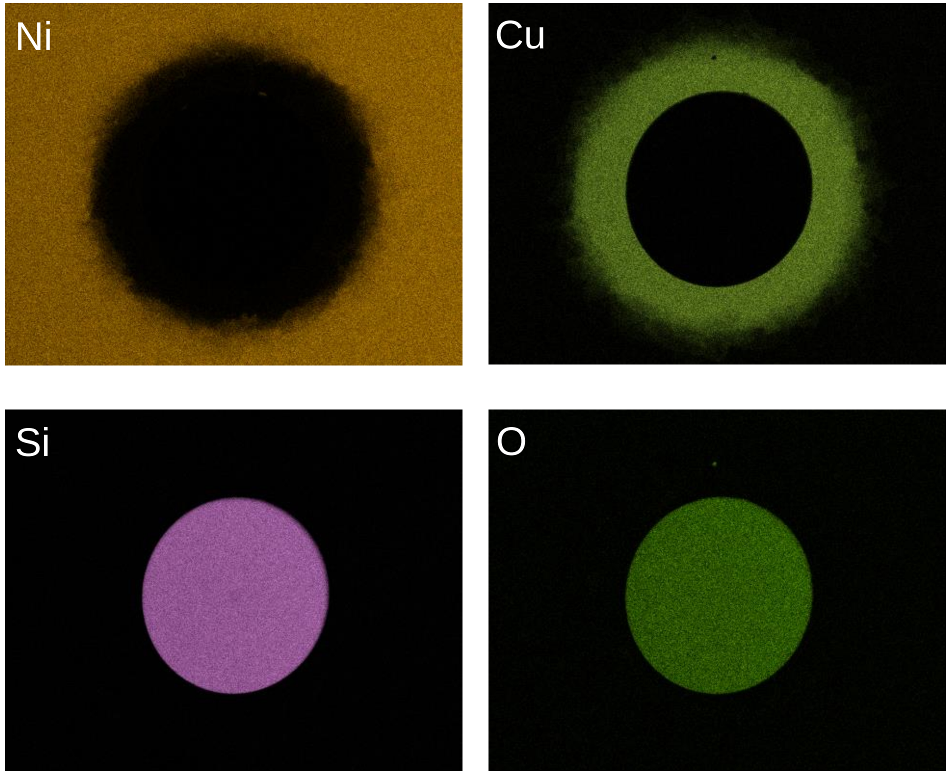

5. Conclusions and Next Steps

Conclusions:

- Fiber optic sensors were successfully integrated into stainless steels and nickel via the developed embedding technique.
- Optical attenuation of sapphire fibers due to embedding was measured to be 0.3-1.86dB and was linked to the fabrication conditions.
- Insertion loss from the embedded fused silica fiber in nickel block is 0.43~0.52 dB (similar to a fiber connector), caused by strain/stress on the embedded fibers.
- A well-bonded interface with interdiffusion across the dissimilar materials was observed. Fibers embedded at optimal conditions passed the leak test.
- Superior tensile properties of the matrix and fiber-matrix integrated materials.
- Demonstrated machinability

5. Conclusions and Next Steps

Next steps

- Evaluate sensing functionality under temperature variations with signal transmitting through the developed fiber optic feedthroughs.
- Near-net shape manufacturing with embedded fiber optic sensors with EFAS. Evaluate sensor integrity, performance, and sensing capabilities.
- Embed magnetostrictive sensors using EFAS. Evaluate embedding performance and demonstrate strain sensing under external load

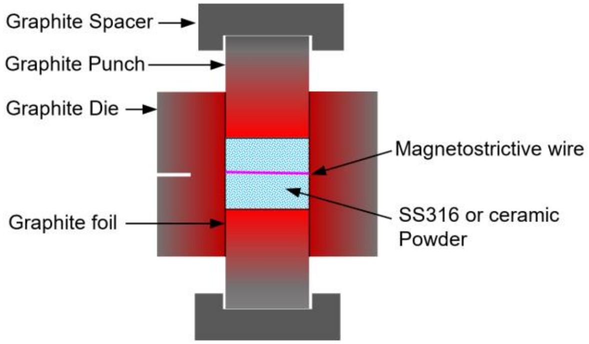

EFAS embedding of magnetostrictive wires

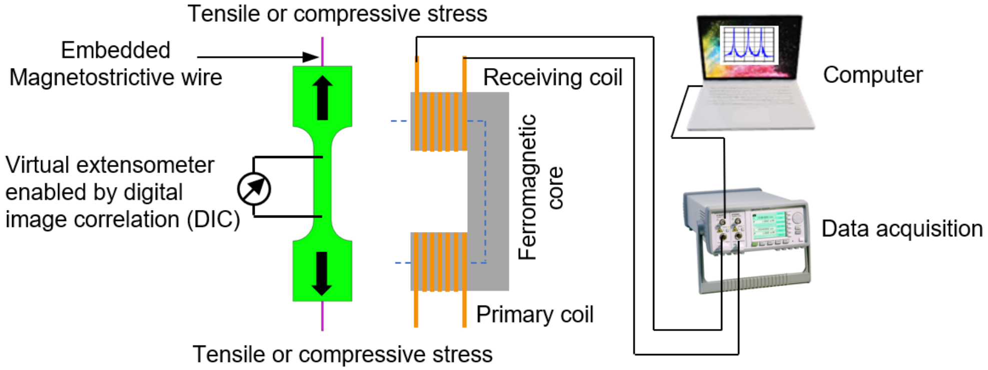

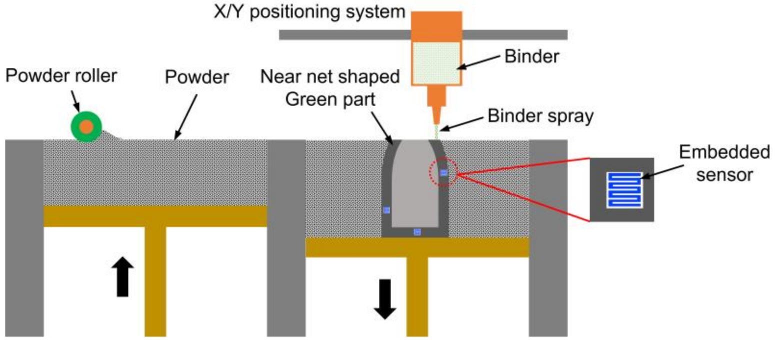

Binder jetting near net shape manufacturing with embedded sensors

Battelle Energy Alliance manages INL for the U.S. Department of Energy's Office of Nuclear Energy. INL is the nation's center for nuclear energy research and development, and also performs research in each of DOE's strategic goal areas: energy, national security, science and the environment.

xinchang.zhang@inl.gov